

UNCLASSIFIED

AD722165

THE ELECTROCHEMICAL AND CORROSION  
BEHAVIOR OF ALUMINUM

By George A. DiBari

Technical Memorandum

File No. TM 703-02

June 18, 1970

Contract N00017-70-C-1407

Copy No. 5

APPROVED  
FOR PUBLIC RELEASE  
DISTRIBUTION UNLIMITED

The Pennsylvania State University  
Institute for Science and Engineering  
ORDNANCE RESEARCH LABORATORY  
University Park, Pennsylvania

Reproduced by  
NATIONAL TECHNICAL  
INFORMATION SERVICE  
Springfield, Va 22151

DISTRIBUTION STATEMENT A  
Approved for public release;  
Distribution Unlimited

DDC  
REF ID: A67116  
APR 26 1971  
C

UNCLASSIFIED

NAVY DEPARTMENT

NAVAL ORDNANCE SYSTEMS COMMAND

92

## ABSTRACT

The electrochemical behavior of high-purity aluminum has been studied to clarify the corrosion behavior of the metal when exposed to oxygen-free and oxygen-saturated saline solutions of varying pH. The mixed or corrosion potential,  $E_M$ , of the electropolished high-purity aluminum decreases as the pH is increased except in the intermediate pH range (4 to 8) where  $E_M$  increases. A local maximum in the corrosion potential curve as a function of pH is thus observed. The potentiostatic polarization data and controlled-potential weight-loss data obtained at pH 4.0 suggest that the rate of dissolution of high-purity aluminum is nearly independent of electrode potential over a fairly wide range, relatively insensitive to the presence of dissolved oxygen in the electrolyte, and highly sensitive to changes in pH. Based on the potentiostatic data, a corrosion diagram believed to be valid from pH 0 to pH 14 has been constructed. The corrosion diagram is consistent with the observed relation between  $E_M$  and pH, and also yields a curve for the rate of dissolution of aluminum as a function of pH. The rate of dissolution of high-purity aluminum increases slightly between pH 0 and 4, decreases between pH 4 and 8, and increases from pH 8 to 14. The minimum at pH 8 may be the point at which the rate of formation of aluminum hydroxide on the electrode surface equals the rate of formation of the aluminate ion.

## TABLE OF CONTENTS

	<u>Page</u>
ACKNOWLEDGMENTS . . . . .	11
LIST OF TABLES. . . . .	iv
LIST OF FIGURES . . . . .	v
I. INTRODUCTION . . . . .	1
II. THEORETICAL BASIS. . . . .	3
Reversible Potentials. . . . .	3
Polarization and Activation Overvoltage. . . . .	8
Mixed Potentials and Self-Polarization . . . . .	11
Exchange Current Density Criterion . . . . .	14
External Polarization and Corrosion Diagrams . . . . .	15
Electrochemical Mechanism of Corrosion . . . . .	18
III. REVIEW OF PERTINENT LITERATURE . . . . .	19
Polarization Characteristics of Aluminum . . . . .	19
Corrosion Behavior of Aluminum . . . . .	26
IV. EXPERIMENTAL DETAILS . . . . .	29
Materials and Specimen Preparation . . . . .	29
Corrosion Potential Measurements . . . . .	31
Potentiostatic Polarization Measurements . . . . .	32
Controlled-Potential Weight-Loss Experiments . . . . .	35
V. RESULTS AND DISCUSSION . . . . .	36
Corrosion Potentials of High-Purity Aluminum . . . . .	36
Polarization Behavior at pH 4.0. . . . .	45
Controlled-Potential Weight-Loss Data. . . . .	57
Interpretation of the Results. . . . .	61
Summary and Conclusions. . . . .	75
BIBLIOGRAPHY. . . . .	79

## LIST OF TABLES

<u>Table</u>		<u>Page</u>
1	SUMMARY OF CONTROLLED-POTENTIAL WEIGHT- LOSS EXPERIMENTS . . . . .	60

## LIST OF FIGURES

<u>Figure</u>		<u>Page</u>
1	SCHEMATIC REPRESENTATION OF THE ENERGY LEVELS OF METAL IONS IN THE LATTICE AND IN SOLUTION: (A) INITIAL STATE AND (B) AT EQUILIBRIUM. . . . .	4
2	SCHEMATIC OF THE EFFECT OF POLARIZATION ON THE ENERGY LEVELS OF METAL IONS IN THE LATTICE AND IN SOLUTION: (A) ANODIC POLARIZATION, (B) EQUILIBRIUM, (C) CATHODIC POLARIZATION . . . . .	9
3	SCHEMATIC OF THE SELF-POLARIZATION PROCESS WHEN TWO REACTIONS ARE OCCURRING SIMULTANEOUSLY. . . . .	13
4	RELATION BETWEEN SELF-POLARIZATION AND EXTERNAL POLARIZATION CURVES: (A) SELF POLARIZATION (B) EXTERNAL POLARIZATION . . . . .	17
5	SCHEMATIC DIAGRAM OF CATHODIC POLARIZATION OF HIGH-PURITY ALUMINUM IN DEOXYGENATED AND AIR-SATURATED 0.2 N SODIUM CHLORIDE, pH 6.2, 24°C . . . . .	20
6	SCHEMATIC DIAGRAM OF EXPERIMENTAL SET-UP. . . . .	33
7	CORROSION POTENTIALS OF ELECTROPOLISHED HIGH-PURITY ALUMINUM AS A FUNCTION OF pH IN AIR-SATURATED 0.056N SODIUM SULFATE AT ROOM TEMPERATURE: ● INITIAL VALUES; ○ ONE HOUR VALUES . . . . .	38
8	CORROSION POTENTIALS OF ELECTROPOLISHED HIGH-PURITY ALUMINUM AS A FUNCTION OF pH IN AIR-SATURATED 0.5N SODIUM CHLORIDE AT ROOM TEMPERATURE: ○ INITIAL VALUES; ● ONE HOUR VALUES . . . . .	39
9	CORROSION POTENTIALS OF ELECTROPOLISHED HIGH-PURITY ALUMINUM AS A FUNCTION OF pH IN AIR-SATURATED 0.5N SODIUM CHLORIDE AND 0.056N SODIUM SULFATE AT ROOM TEMPERATURE: ○ INITIAL VALUES; ● ONE HOUR VALUES . . . . .	40
10	CORROSION POTENTIALS OF ETCHED HIGH-PURITY ALUMINUM AS A FUNCTION OF pH IN AIR-SATURATED 0.5N SODIUM CHLORIDE AT ROOM TEMPERATURE: ○ INITIAL VALUES; ● ONE HOUR VALUES . . . . .	41

## LIST OF FIGURES (CONTINUED)

<u>Figure</u>		<u>Page</u>
11	CORROSION POTENTIALS OF ETCHED HIGH-PURITY ALUMINUM AS A FUNCTION OF pH IN AIR-SATURATED 0.056N SODIUM SULFATE AT ROOM TEMPERATURE: O INITIAL VALUES, ● ONE HOUR VALUES . . . . .	42
12	CORROSION POTENTIALS OF ETCHED HIGH-PURITY ALUMINUM AS A FUNCTION OF pH IN AIR-SATURATED 0.5N SODIUM CHLORIDE AND 0.056N SODIUM SULFATE AT ROOM TEMPERATURE: O INITIAL VALUES, ● ONE HOUR VALUES. . .	43
13	DUPLICATE RESULTS OF CATHODIC POLARIZATION OF ELECTROPOLISHED HIGH-PURITY ALUMINUM IN DEAERATED 0.5N SODIUM CHLORIDE AT 30°C AND pH 4.0 . . . . .	46
14	TRIPPLICATE RESULTS OF CATHODIC POLARIZATION OF ELECTROPOLISHED HIGH-PURITY ALUMINUM IN AIR-SATURATED 0.5N SODIUM CHLORIDE AT 30°C AND pH 4.0, INCLUDING A RESULT IN THE ABSENCE OF OXYGEN (DOTTED LINE) . . . . .	47
15	CATHODIC POLARIZATION OF HIGH-PURITY ALUMINUM IN 0.5N SODIUM CHLORIDE AT 30°C AND pH 4.0: O AFTER 24 HOURS EQUILIBRATION IN THE PRESENCE OF OXYGEN; --. AFTER 1 HOUR EQUILIBRATION IN THE PRESENCE OF OXYGEN; --- AFTER 1 HOUR EQUILIBRATION IN THE ABSENCE OF OXYGEN . . . . .	49
16	CATHODIC POLARIZATION OF HIGH-PURITY ALUMINUM IN AIR-SATURATED 0.5N SODIUM CHLORIDE AT 30°C AND pH 4.0: O NITRIC ACID-TREATED SPECIMEN; --. ELECTROPOLISHED AND POLARIZED IN THE PRESENCE OF OXYGEN; --- ELECTROPOLISHED AND POLARIZED IN THE ABSENCE OF OXYGEN. . . . .	51
17	CATHODIC POLARIZATION OF HIGH-PURITY ALUMINUM IN DEAERATED 0.5N SODIUM CHLORIDE AT 30°C AND pH 4.0: --- FIRST DETERMINATION, O SECOND DETERMINATION ON SAME SPECIMEN, THE CIRCUIT BEING OPENED BETWEEN DETERMINATIONS. . . . .	52
18	CATHODIC POLARIZATION OF HIGH-PURITY ALUMINUM IN AIR-SATURATED 0.5N SODIUM CHLORIDE AT 30°C AND pH 4.0: O FIRST DETERMINATION; ● SECOND DETERMINATION, THE SPECIMEN BEING POLARIZED FROM -1.6 TO -1.12 VOLTS WITHOUT OPENING THE CIRCUIT BETWEEN DETERMINATIONS. . . . .	53

## LIST OF FIGURES (CONTINUED)

<u>Figure</u>		<u>Page</u>
19	CATHODIC AND ANODIC POLARIZATION OF HIGH-PURITY ALUMINUM IN AIR-SATURATED 0.5N SODIUM CHLORIDE AT 30°C AND pH 4.0: ○ FIRST DETERMINATION OF CATHODIC AND ANODIC POLARIZATION; ● SECOND DETERMINATION ON SAME SPECIMEN, THE CIRCUIT BEING OPENED BETWEEN DETERMINATIONS. . . . .	55
20	EFFECT OF REPEATED CATHODIC AND ANODIC POLARIZATION OF HIGH-PURITY ALUMINUM IN DEAERATED 0.5N SODIUM CHLORIDE AT 30°C AND pH 4.0 . . . . .	56
21	COMPARISON OF CONTROLLED-POTENTIAL WEIGHT-LOSS DATA AT pH 4.0 IN AIR-SATURATED 0.5N SODIUM CHLORIDE WITH RESULTS REPORTED BY KUNZE IN DEAERATED BUFFERED 0.5N SODIUM CHLORIDE AT pH 5.0 . . . . .	59
22	POLARIZATION CHARACTERISTICS OF A METAL DISPLAYING STABLE PASSIVE BEHAVIOR: (A) SELF-POLARIZATION CURVES (B) CORRESPONDING EXTERNAL POLARIZATION CURVES. ANODIC CURRENTS INDICATED BY DOTTED LINES . . . . .	62
23	SELF-POLARIZATION CURVES OF HIGH-PURITY ALUMINUM IN 0.5N SODIUM CHLORIDE AS CONSTRUCTED FROM THE EXPERIMENTAL DATA . . . . .	65
24	ESTIMATE OF THE CORROSION RATE - POTENTIAL - pH DIAGRAM OF ELECTROPOLISHED HIGH-PURITY ALUMINUM IN 0.5N SODIUM CHLORIDE . . . . .	70
25	SUMMARY OF CORROSION POTENTIALS OF HIGH-PURITY ALUMINUM AS A FUNCTION OF pH: ELECTROPOLISHED SPECIMENS IN: □ 0.056N SODIUM SULFATE, Δ 0.5N SODIUM CHLORIDE; ○ 0.056N SODIUM SULFATE AND 0.5N SODIUM CHLORIDE; ETCHED SPECIMENS IN: ■ 0.056N SODIUM SULFATE; ▲ 0.5N SODIUM CHLORIDE; AND ● 0.056N SODIUM SULFATE AND 0.5N SODIUM CHLORIDE. . . . .	72
26	ESTIMATE OF THE INITIAL RATE OF DISSOLUTION OF HIGH-PURITY ALUMINUM AS A FUNCTION OF pH IN 0.5N SODIUM CHLORIDE . . . . .	74

## CHAPTER I

### INTRODUCTION

The electrochemical reduction of dissolved oxygen is of fundamental importance in any consideration of the corrosion behavior of metals in aqueous solutions. Dissolved oxygen is present in most practical environments and may act to depolarize the corrosion reaction, thereby increasing the rate of attack. The presence of dissolved oxygen is especially important in neutral salt solutions where the activity of the hydronium ion is low and where discharge of hydrogen proceeds with difficulty on many metal surfaces.<sup>(1)</sup> The rate of corrosion under these conditions is generally determined by the availability of dissolved oxygen.

The rate of corrosion of aluminum, however, is strongly influenced by the oxide film almost always present on its surface. The importance of the passive film is evident in the low rate of corrosion of aluminum in those environments in which the passive film is stable, and the high rate when the film is not stable.<sup>(2)</sup>

The nature of the corrosive attack on aluminum is affected by the existence of the oxide film. The tendency for aluminum to corrode non-uniformly by a pitting-type of attack, especially in near-neutral solutions, is often attributed to localized breakdown of the oxide film.<sup>(3)</sup> A general relationship between the presence of oxide films and the non-uniform dissolution of metals is believed to exist.<sup>(4)</sup>



The passive oxide film on aluminum thus influences the rate of corrosion and the nature of the corrosive attack; hence, the film should affect the rate of reduction of dissolved oxygen and the role of oxygen in the corrosion process.

The objective of the work described in this thesis is to determine the effects of electrode potential, pH, and dissolved oxygen on the electrochemical and corrosion behavior of high purity aluminum. The variation of the corrosion potential with pH has been determined in sodium chloride and sodium sulfate solutions. Cathodic and anodic polarization data were obtained in air-saturated and deaerated solutions of sodium chloride at pH 4.0. Controlled-potential weight-loss data were gathered. The data are interpreted in terms of mixed potential behavior and used to construct corrosion diagrams utilizing techniques described in the literature. (5-8)

## CHAPTER II

### THEORETICAL BASIS

Electrode kinetics, in terms of the current-voltage or polarization characteristics of a system, can provide useful information about the corrosion behavior of metals. The kinetics of corrosion processes will be discussed to indicate the theoretical basis of the experimental approach and to review the main ideas underlying the electrochemical mechanism of the corrosion of metals.

#### Reversible Potentials

The basic similarity between the mechanism of corrosion of metals in aqueous solutions and that by which an electrode potential is established has been pointed out.<sup>(9)</sup> When a metal is immersed in a solution of its ions, there will be a simultaneous transfer of ions in both directions across the interface. Since the interface represents an energy barrier, the transfer reactions across the metal-solution interface can be discussed in terms of transition state or absolute reaction rate theory.<sup>(10)</sup>

Consider the energy-distance relationships in Figure 1(A) where the energy is expressed in units of  $nFE$  volt-coulombs. The ions in the lattice must acquire an anodic activation energy,  $nFE_c^\ddagger$ , to go into solution, while the metal ions in solution must acquire the cathodic activation energy,  $nFE_c^\ddagger$ , to enter the lattice.

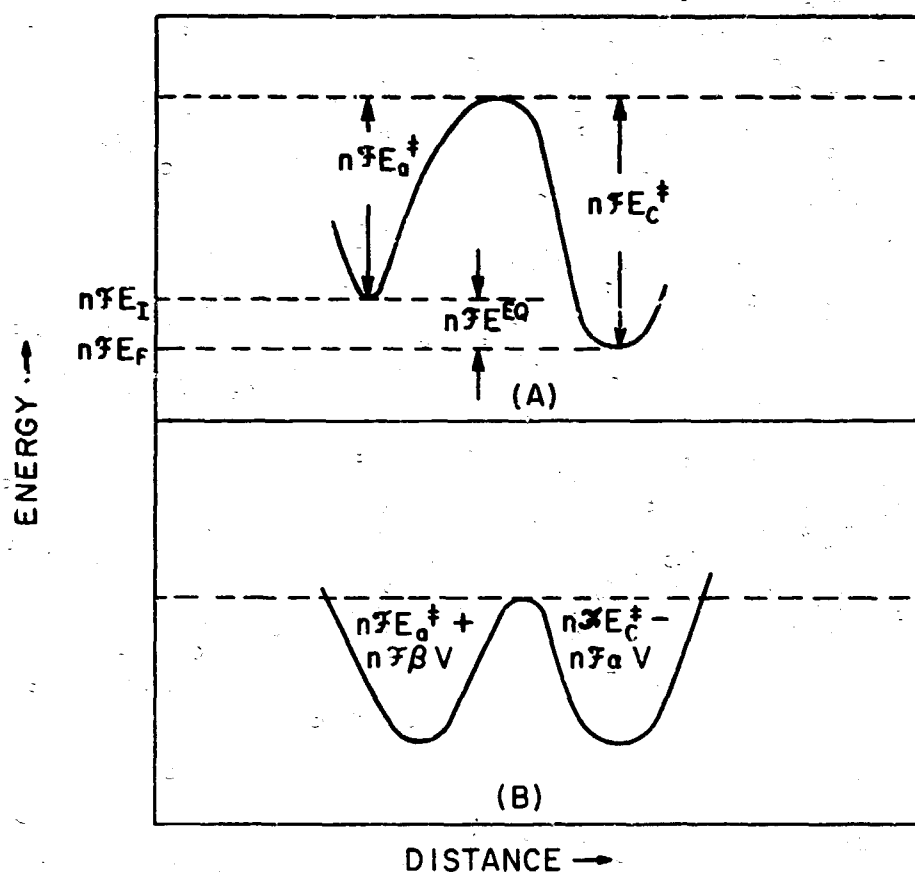


FIGURE 1 SCHEMATIC REPRESENTATION OF THE ENERGY LEVELS OF METAL IONS IN THE LATTICE AND IN SOLUTION: (A) INITIAL STATE AND (B) AT EQUILIBRIUM.

As depicted in the figure,  $E_a^\ddagger < E_c^\ddagger$ , and initially there will be a greater tendency for metal ions to enter the solution than to leave it. The result is that the metal acquires a negative charge, the solution a positive one. A potential difference,  $V$ , is thus created at the metal-solution interface. For the case under consideration,  $V$  acts to hinder the exchange reaction in the anodic direction and to aid it in the opposite direction. The potential difference effective in the cathodic direction can be set equal to  $\alpha V$ , that in the anodic direction to  $\beta V$ , where  $\alpha$  and  $\beta$  are termed transfer coefficients, and  $\alpha + \beta = 1$ .

The equilibrium situation can then be depicted as in Figure 1(b). The anodic activation energy has been increased by  $nF\beta V$ . The cathodic activation energy has been decreased by  $nF\alpha V$ .

At equilibrium.

$$E_a^\ddagger + \beta V = E_c^\ddagger - \alpha V$$

and rearranging:

$$E_c^\ddagger - E_a^\ddagger = (\alpha + \beta)V$$

Since  $\alpha + \beta = 1$  and  $E_c^\ddagger - E_a^\ddagger = E^{eq}$ ,

$$E^{eq} = V, \quad (1)$$

i.e., the equilibrium potential,  $E^{eq}$ , is equal to the potential difference at the metal-solution interface.

The equilibrium potential is a constant at constant temperature and metal ion activity. The rates of the exchange reaction in the anodic direction,  $i_a^\ddagger$ , and in the cathodic direction,  $i_c^\ddagger$ , are given by:

$$i_a^\ddagger = k_1 \cdot \exp[nF(E_a^\ddagger + \beta V)/RT] \quad (2)$$

and

$$i_c^\ddagger = k_2 \cdot a_{M^{n+}} \cdot \exp[nF(E_c^\ddagger - \alpha V)/RT] \quad (3)$$

where  $k_1$  and  $k_2$  are constants independent of concentration, and  $a_{M^{n+}}$  is the activity of the metal ions in solution.

At equilibrium:

$$i_a^\ddagger = i_c^\ddagger \quad (4)$$

and substituting Equations (2) and (3) in Equation (4), rearranging, and eliminating the exponentials:

$$\ln \frac{k_1}{k_2} + \frac{nF}{RT} (E_a^\ddagger - E_c^\ddagger) + \frac{nFV}{RT} = \ln a_{M^{n+}} \quad .$$

Since the first two terms on the left are constant, this can be written:

$$V = k + \frac{RT}{nF} \ln a_{M^{n+}}$$

and, since  $V = E^{eq}$ , the equilibrium electrode potential is a constant at constant temperature and metal ion activity.

When

$$a_{M^{n+}} = 1 ,$$

$$k = E_O^{eq} ,$$

where  $E_O^{eq}$  is the standard reversible potential.

In general:

$$E^{eq} = E_O^{eq} + \frac{RT}{nF} \ln a_{M^{n+}}$$

which is the Nernst equation. The equation indicates that, at 25°C, every ten-fold shift in the activity of the metal ions will shift the potential by about 58 millivolts for a univalent charge ( $n=1$ ). In essence, the Nernst equation is the practical criterion for reversibility; i.e., an electrode which acts as predicted by the equation is said to be a reversible one.

In the above discussion, we have assumed that the metal cations are the only species exchanged at the interface. However, in other systems electrons are exchanged. This will be possible when the energy levels for the electrons near the Fermi level in the metal overlap the energy levels of electron acceptors in the solution. The criterion for reversibility remains the same whether metal cations or electrons are exchanged.

What has this to do with the corrosion of metals? Corrosion involves the transfer of metal ions from the lattice to the solution, so that a process similar to the one pictured above must occur. For corrosion to predominate, transfer of metal ions from the lattice to the solution must occur at a greater rate than the reverse

process; i.e.,

$$i_a > i_c$$

Corrosion, therefore, represents a departure from equilibrium, and the electrode potential must be shifted from its equilibrium value.

### Polarization and Activation Overvoltage

If the equilibrium potential of an electrode is altered, the electrode is said to be polarized. Polarization affects the energy-distance relationships as shown schematically in Figure 2.

For the case of anodic polarization, we can write:

$$i_a = k_1 \cdot \exp[nF(E_a^\ddagger - \beta(E - E^{eq}))/RT]$$

and

$$i_c = k_2 \cdot a_{M^{n+}} \cdot \exp[nF(E_c^\ddagger + \alpha(E - E^{eq}))/RT]$$

where  $E$  is the electrode potential and  $(E - E^{eq})$  is the amount by which the potential has been shifted from the equilibrium value.

It is convenient to define the term, activation overvoltage, as follows:

$$\eta_a = E - E^{eq}$$

so that, on anodic polarization, the activation overvoltage is always positive and, on cathodic polarization, it is always negative.

When the activation overvoltage is zero:

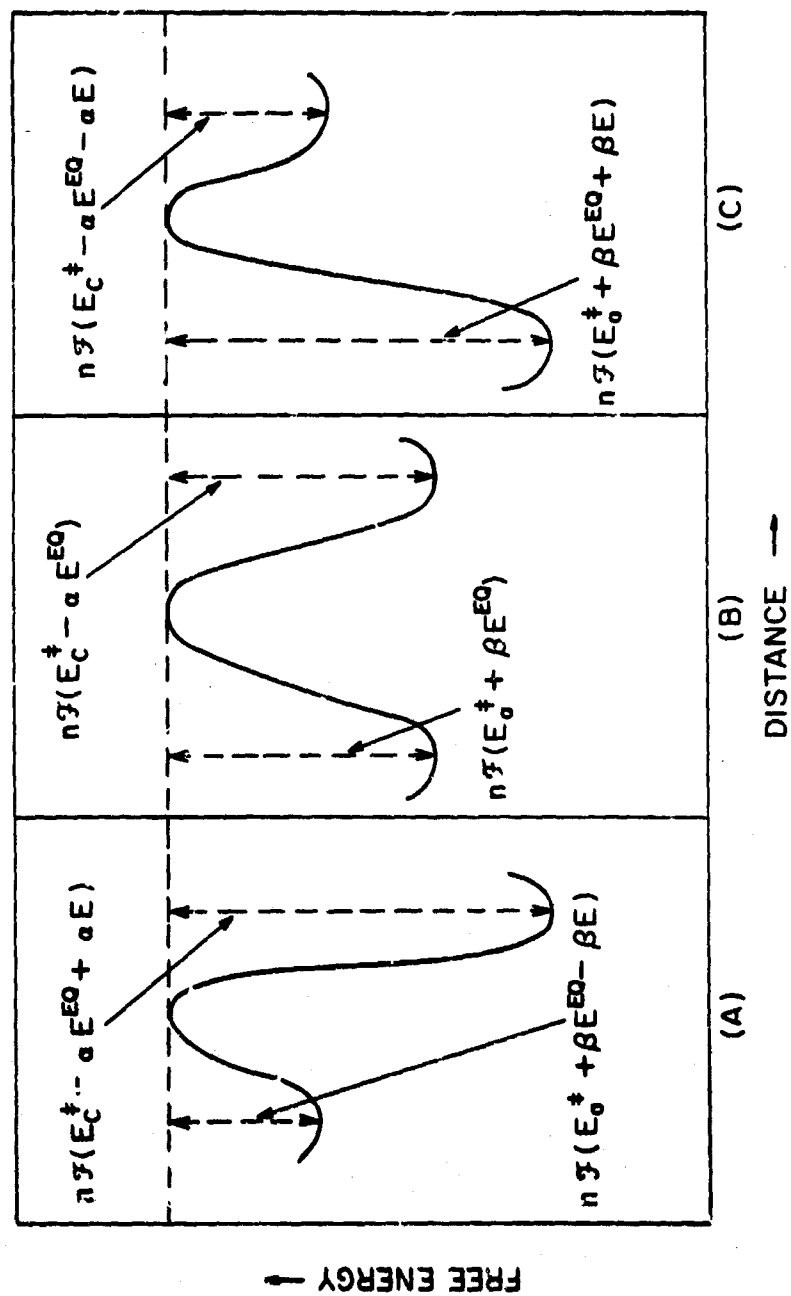


FIGURE 2 SCHEMATIC OF THE EFFECT OF POLARIZATION ON THE ENERGY LEVELS OF METAL IONS IN THE LATTICE AND IN SOLUTION: (A) ANODIC POLARIZATION, (B) EQUILIBRIUM, (C) CATHODIC POLARIZATION



$$E = E^{eq} ,$$

and

$$\bar{i}_a = \bar{i}_c = i_o ,$$

where  $i_o$ , the exchange current density, is the rate of the exchange reaction at equilibrium, and is dependent on the activities of the ionic species.

The rate equations can then be written:

$$\bar{i}_a = i_o \exp[nF\beta\eta_a/RT]$$

and

$$\bar{i}_c = i_o \exp[-nF\alpha\eta_a/RT] ,$$

where the signs of the exponentials have been made consistent with the above definition of activation overvoltage; i.e.,  $\bar{i}_a$  must increase on anodic polarization when  $\eta_a$  is positive, and  $\bar{i}_c$  must increase on cathodic polarization when  $\eta_a$  is negative.

The net current,  $i$ , is given by:

$$i = \bar{i}_c - \bar{i}_a ,$$

that is,

$$i = i_o [\exp(-nF\alpha\eta_a/RT) - \exp(nF\beta\eta_a/RT)] . \quad (5)$$

At overvoltages greater than -0.050 volts, Equation (5) becomes:

$$i_c = i_o \exp(-nF\alpha\eta_a/RT) , \quad (6)$$

and at greater than 0.050 volts:

$$i_a = -i_o \exp(nF\beta\eta_a/RT) , \quad (7)$$

where  $i_c$  and  $i_a$  are cathodic and anodic currents, respectively.

Anodic currents are arbitrarily assigned a negative sign. Equations (6) and (7) are forms of Tafel's equation.

The effect of disturbing the equilibrium electrode potential is to cause a net current to flow. At sufficiently high values of applied potential, the reverse processes are suppressed and a cathodic or anodic current results. A potential applied anodically results in a net transfer of metal ions from the lattice to the solution, and the metal electrode undergoes corrosion.

#### Mixed Potentials and Self-Polarization

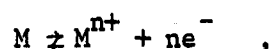
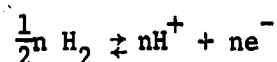
The effects of polarization have been described above without indicating by what process the electrode potential is shifted from its equilibrium value. The electrode potential can be altered by externally applied potentials or by a process called self-polarization.

Self-polarization occurs because two or more electrochemical reactions can proceed simultaneously at the surface of an electrode immersed in a solution. The reactions proceed independently of each other at a common electrode potential. Since only one electrode is involved and electroneutrality must be maintained, the sum of the rates of the individual reactions must be zero; i.e.,

$$i_{\text{Total}} = \sum_{i=1}^x i_i = 0, \quad (8)$$

where the summation involves equations of the form of Equation (5).

Consider the specific case in which the following two reactions are taking place simultaneously:



i.e., the oxidation and reduction of hydrogen and metal ions proceed simultaneously at the metal surface. If we perform the summation indicated in Equation (8) and assume that  $\alpha_1 = \alpha_2 = \alpha$ , it can be shown that the common electrode potential would be given by: (5)

$$E_m = \frac{RT}{nF} \ln \frac{i_{0,1} \exp(nF\alpha E_1^{\text{eq}}/RT) + i_{0,2} \exp(nF\alpha E_2^{\text{eq}}/RT)}{i_{0,1} \exp(-nF\beta E_1^{\text{eq}}/RT) + i_{0,2} \exp(-nF\beta E_2^{\text{eq}}/RT)}, \quad (9)$$

where  $i_{0,1}$  and  $i_{0,2}$  are the exchange current densities, and  $E_1^{\text{eq}}$  and  $E_2^{\text{eq}}$  are the thermodynamically reversible potentials of the hydrogen and metal redox reactions, respectively.  $E_m$ , the common electrode potential, is commonly called the mixed potential.  $E_m$  is also known as the compromise, reaction, or corrosion potential.

The self-polarization process and the manner by which the mixed potential is established is shown schematically in Figure 3.

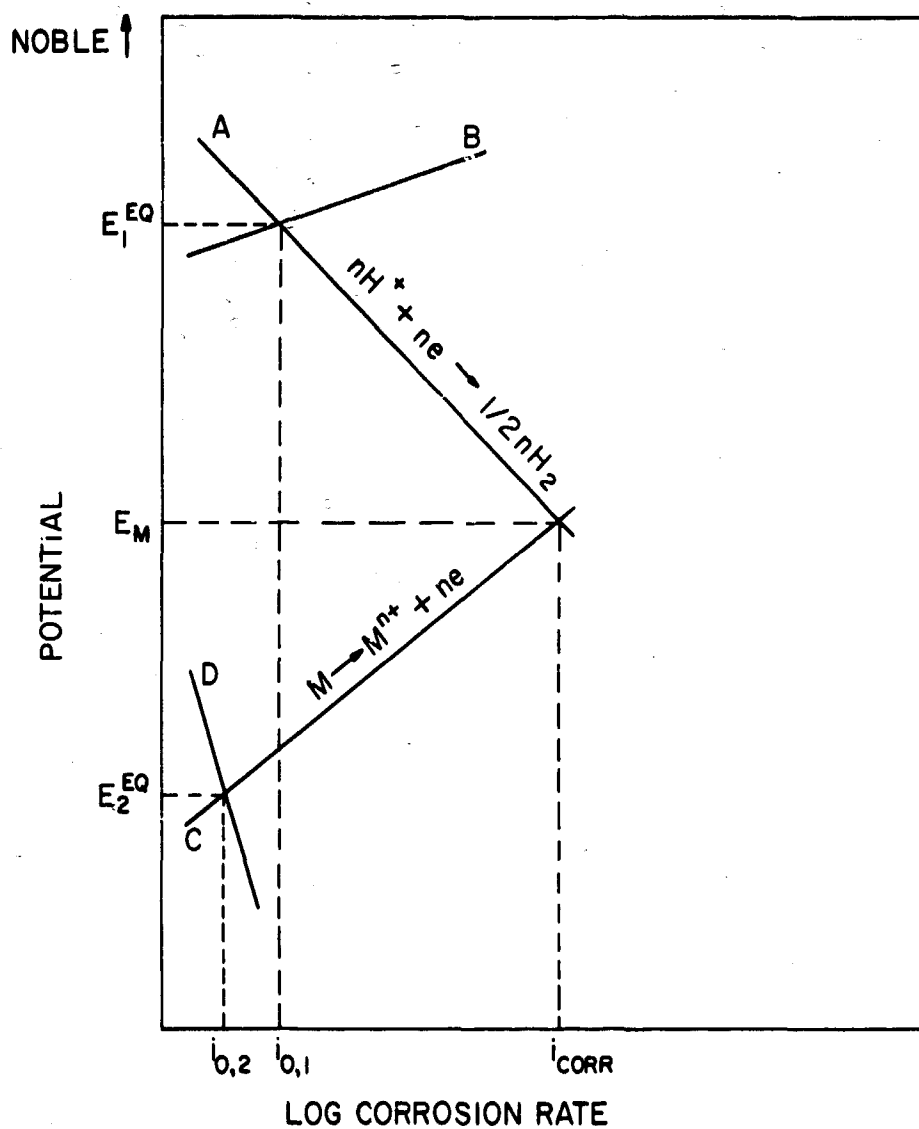


FIGURE 3 SCHEMATIC OF THE SELF-POLARIZATION PROCESS WHEN TWO REACTIONS ARE OCCURRING SIMULTANEOUSLY

The figure is constructed from equations of the form of Equations (6) and (7) where the absolute values of the anodic currents are plotted. The point at which the total current is zero is found by extending curves A and C to their point of intersection. The coordinates of the point of intersection are the mixed potential,  $E_m$ , and the rate of corrosion  $i_{\text{corr}}$ . That this is analogous to the effect of an applied potential is evident from the fact that  $E_m > E_2^{\text{eq}}$  and the electrode is anodic to its equilibrium potential. Therefore, a net transfer of metal ions from the lattice to the solution occurs as a result of the self-polarization process.

#### Exchange Current Density Criterion

When  $i_{0,1} \gg i_{0,2}$ , Equation (9) reduces to:

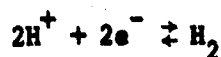
$$E_m = E_1^{\text{eq}}$$

and the electrode establishes a reversible potential determined by the  $\text{H}_2/\text{H}^+$  equilibrium. Alternatively, when  $i_{0,2} \gg i_{0,1}$ , Equation (9) becomes:

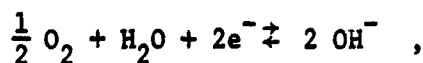
$$E_m = E_2^{\text{eq}}$$

and the electrode potential is determined by the  $\text{M}/\text{M}^{n+}$  equilibrium. Thus, the relative magnitude of the exchange current density values determines whether the electrode potential is reversible or mixed.

In practical systems, equilibria such as



and



representing the reduction of hydrogen ions and of oxygen, respectively, are possible. If the exchange current density values for these equilibria are equal to the value of the  $\text{M}/\text{M}^{n+}$  equilibrium, the electrode potential will be mixed and will depend on pH and  $p\text{O}_2$ . As shown above, the electrode will be anodic and will corrode. The importance of cathodic reactions such as the reduction of hydrogen ions and of oxygen stems from the above considerations.

#### External Polarization and Corrosion Diagrams

A metal electrode will self-polarize immediately on immersion in a solution. The electrode will establish a mixed potential which can be measured directly. The rate of corrosion can be determined from weight-loss data as a function of time or by an external polarization process.

To determine the rate of corrosion by an external polarization process, an inert electrode, usually platinum, is placed in the same solution with the electrode being studied. If an EMF is now imposed on the system, the mixed potential of the electrode will be altered and current will flow through the cell. Equation (8) no longer applies. Instead we can write:

$$I = \sum_{i=1}^n i_i \neq 0 .$$

where  $I$  is the external current which flows through the cell. If

the values of the current and the potential are recorded, a current-voltage curve can be constructed for the system. The data can be used to determine the rate of corrosion and to construct corrosion diagrams similar to the one drawn in Figure 3.

The relation between external polarization and self-polarization curves is illustrated in Figure 4, and is given by

$$I = |i_c + i_a| ,$$

where  $i_c$  and  $i_a$  are given by equations of the form of Equations (6) and (7). Self-polarization or corrosion diagrams can therefore be constructed from external polarization data.

The external polarization data may be considerably more difficult to analyze and resolve into the corresponding corrosion diagram than the rather simple example used for illustration. For example, concentration and resistance polarization effects can obscure linear relationships. Concentration polarization can occur when a reductant or oxidant is present in small amounts in solution. Resistance polarization can occur when an oxide film or corrosion product is present on the electrode surface. Both phenomena limit the amount of current that can flow and cause the current-voltage curve to depart from linearity at high overvoltage values. Impurities in solution, agitation, the rate of change of potential and other factors influence the shape of the external polarization curve and may make interpretation difficult. Despite these difficulties, the above basic principles appear valid.

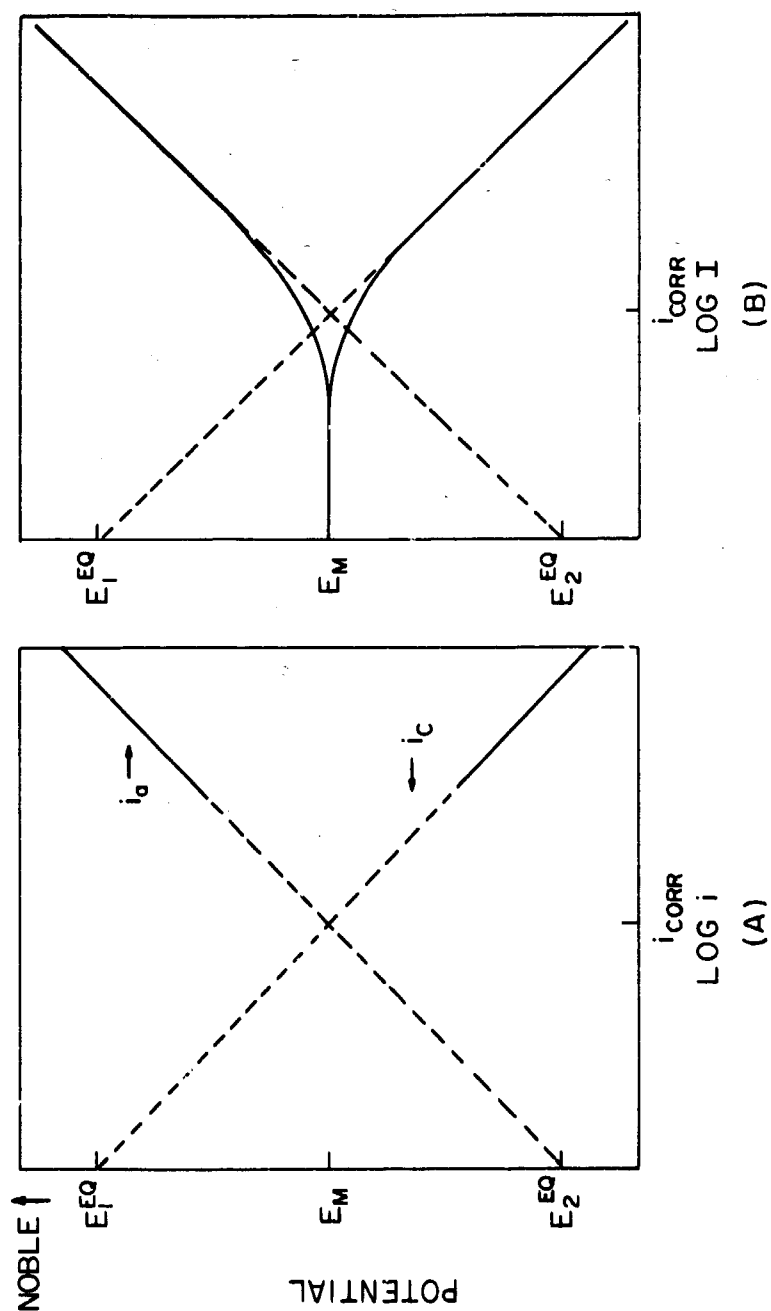


FIGURE 4 RELATION BETWEEN SELF-POLARIZATION AND EXTERNAL POLARIZATION  
CURVES: (A) SELF-POLARIZATION (B) EXTERNAL POLARIZATION



### Electrochemical Mechanism of Corrosion

In summary, the mechanism of corrosion of metals in aqueous solution is fundamentally the same as that by which a reversible electrode potential is established. In the case of the reversible electrode potential, a single process is taking place at the electrode, the exchange reaction involves oxidized and reduced forms of the same chemical species, and changes in the electrode potential can be predicted from the Nernst equation.

In the case of an electrode undergoing corrosion, two or more electrode processes must occur simultaneously, the exchange reaction involves oxidized and reduced forms of different chemical species, and the mixed potential is dependent on the exchange current density values for each of the possible electrode reactions. The rate of corrosion depends on the extent to which the metal is made anodic by the various electrode reactions taking place. The process by which the electrode establishes a mixed potential has been termed self-polarization. It is possible to construct corrosion diagrams from current-voltage data and to determine rates of corrosion.

## CHAPTER III

### REVIEW OF PERTINENT LITERATURE

The polarization characteristics of aluminum in air-saturated and deoxygenated solutions are discussed below. After reviewing the available polarization data, corrosion studies dealing with the effect of pH,  $pO_2$ , and oxide-films on the rate of dissolution of aluminum are described.

#### Polarization Characteristics of Aluminum

Few comprehensive studies of the effect of dissolved oxygen on the polarization characteristics of aluminum are available. Haynie and Ketcham, however, were concerned with the effect of dissolved oxygen and obtained polarization data in air-saturated and deoxygenated solutions using high-purity (99.9957%) aluminum.<sup>(11)</sup> The electrodes were cathodically polarized in 0.2N sodium chloride at 24°C and at a pH of 6.2. Oxygen was excluded by bubbling nitrogen through the solution. A schematic diagram of the results is given in Figure 5. The shapes of the curves are similar in each case; however, the limiting current density, i.e., the flat portion of the curve, is greater in the absence of oxygen.

Haynie and Ketcham conclude that the limiting current density is not dependent on the rate of reduction of oxygen but is determined by the rate of reduction of hydrogen ions. Moreover, the absence of dissolved oxygen results in an increase in the rate

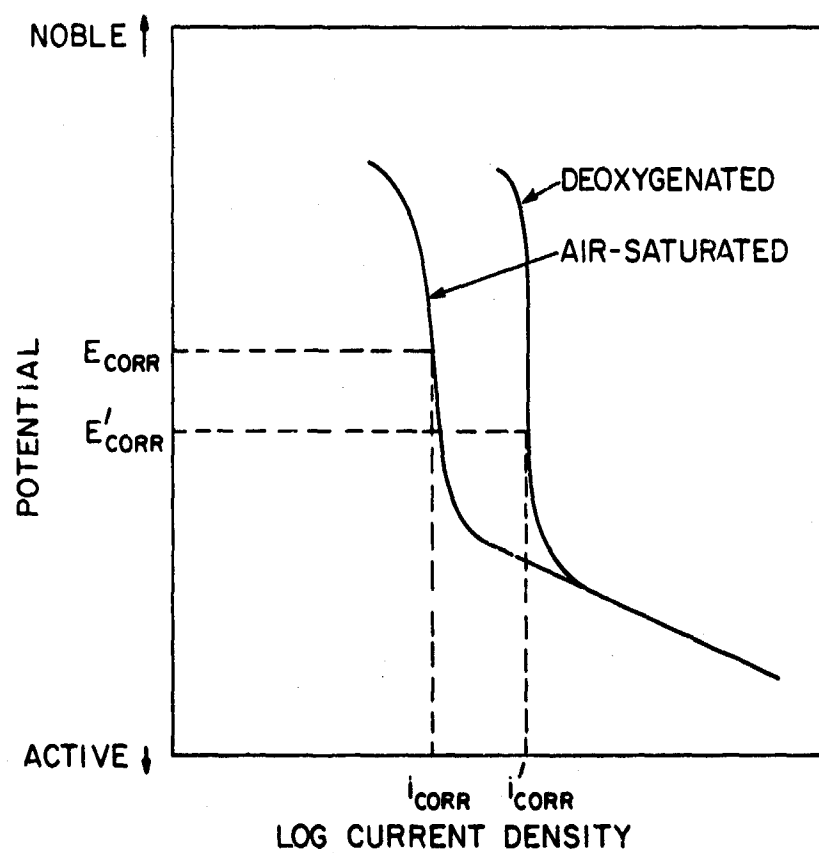


FIGURE 5 SCHEMATIC DIAGRAM OF CATHODIC POLARIZATION OF HIGH-PURITY ALUMINUM IN DEOXYGENATED AND AIR-SATURATED 0.2N SODIUM CHLORIDE, pH 6.2, 24°C

at which hydrogen is reduced, and the authors speculate that the oxide film increases in porosity in the absence of oxygen. The implication is that the corrosion rate of high-purity aluminum is greater in the absence than in the presence of oxygen. The result is noteworthy because it is opposite to the effect observed with iron and nickel. (6), (12)

It is also contrary to the effects observed with aluminum alloys 3003 and 6061. Koebler and Evans, utilizing electrochemical techniques, found that dissolved oxygen doubled the rate of corrosion of aluminum alloy 3003 in a pH 3.5 citrate buffer. (13) The corrosion rate of aluminum alloy 6061 in seawater was three to four times greater in the presence of oxygen than in its absence. (14) Thus the influence of oxygen appears to be dependent on the purity and composition of the aluminum.

A substantial amount of information is available on the polarization behavior of aluminum in deoxygenated acidic solutions. The corrosion potentials of high-purity aluminum in deoxygenated solutions of salts of the three common mineral acids in the pH range 0 to 3.0 are given by an equation of the form:

$$E_{Al} = K + \frac{RT}{nF} \ln a_{H^+},$$

i.e., the corrosion potential of aluminum varies with pH in the same way as does the potential of a hydrogen electrode, where K is a constant dependent on the anion in solution. (15)

The reported cathodic polarization curves initially show a region of little change of potential with the logarithm of the current density, followed by a region of linear variation. At pH 2.25 in a sodium chloride solution and 3.75 in a sodium sulfate solution, the linear portion of the curves was followed by a region of rapid fall of potential with current density characteristic of concentration or resistance polarization effects. The slopes of the linear portion of the curve varied from 0.15 to 0.197 in the solutions tested and were higher than those for iron and nickel which are about 0.10 under similar conditions. Goulding and Downie also demonstrated that the corrosion rate determined by extrapolation of the linear portion of the curve agreed with the rate of increase of aluminum ions in solution, confirming that the rate of corrosion could be determined from external polarization data.

The anodic polarization of high-purity aluminum in aqueous solutions of chlorides and bromides has also been studied.<sup>(16)</sup> The electrode potential changes only slightly on anodic polarization. At about -0.8 volt versus the saturated calomel electrode (SCE), the current rises sharply and reaches a maximum value at -0.7 volt versus SCE. Thereafter, the current remains constant over a broad potential range. The critical potential (about -0.7 volt versus SCE) is associated with the onset of pitting. In sulfate solutions containing no halides, the rapid rise in current at -0.8 volt (SCE) is not observed. Instead, the current rises smoothly to a maximum value which remains constant over a broad potential range.<sup>(17)</sup>

The effect of anodic oxide films on the cathodic and anodic polarization of aluminum was determined in deaerated chloride solution at pH 0-3.<sup>(18)</sup> The initial values of the electrode potential were in the range -200 to -400 mv. After allowing the electrode to equilibrate with the solution, the final rest potentials were approximately -1.0 volt and varied with the pH of the solution. The Tafel slopes on cathodic polarization at pH 0 ranged from 0.12 to 0.18 volt, and were not significantly different from the slopes obtained with chemically polished or electropolished specimens. On cathodic polarization at current densities of about 100  $\mu\text{A}/\text{cm}^2$ , the potential changed rapidly to a minimum of -2.26 volts. The anodic polarization curves of anodized and potential-equilibrated aluminum specimens were reportedly the same no matter what the initial oxide-film thickness.

If the electrodes are not equilibrated with the solution, the anodic polarization data are sensitive to film thickness. Using a fixed and probably arbitrary rate of polarization, Jones<sup>(19)</sup> showed that the anodic current decreased with increasing film thickness. At constant film thickness, the anodic current increased with increasing temperature. The plot of the logarithm of the current and reciprocal temperature was linear allowing calculation of an activation energy value from the slope of the curve. The slopes of the curves were independent of film thickness.

The electrochemical behavior of aluminum in solutions containing a variety of oxidation-reduction systems was studied by

Petrocelli. (20), (21), (22) The experimental results indicate that the electrochemical behavior of pure aluminum may be interpreted by the theory of the mixed potential. He also suggested that aluminum is generally covered by a thin, compact continuous film of amorphous oxide which has a tendency to become thinner on cathodic polarization.

Kunze has also interpreted the electrochemical behavior of aluminum in terms of mixed potential theory.<sup>(23)</sup> He studied the behavior of high-purity aluminum in deaerated solutions of 0.5M NaCl buffered at pH 5.0 with 0.1M sodium citrate. He concluded that aluminum behaved as a bielectrode with metal dissolution as the anodic process and hydrogen discharge as the cathodic process. At -1.6 volts versus SCE, the current rose rapidly on cathodic polarization. Kunze suggests that the electrode reaction shifts from the solution-metal oxide interface to the metal-metal oxide interface at that potential. The phenomenon may be associated with the rapid change in potential observed by Diggle, Goulding and Downie<sup>(18)</sup> on cathodic polarization above  $100 \mu\text{A}/\text{cm}^2$  and may be consistent with Petrocelli's observation that the oxide film becomes thinner on cathodic polarization.

In summary, the available data on the polarization behavior of aluminum suggest that:

1. The presence of dissolved oxygen in near-neutral solutions reduces the rate of corrosion of high-purity aluminum. This must be reconciled with the fact that dissolved oxygen often increases the rate of corrosion of other metals as well as aluminum alloys.

2. In deaerated solutions, the electrode potentials of aluminum behave in the same way as does the potential of a hydrogen electrode, at least from pH 0 to pH 3.0.
3. The cathodic polarization curves in stagnant deaerated solutions are characterized by a linear portion where potential changes rapidly with current density. It is not clear whether the latter is caused by concentration or resistance polarization effects. There is a characteristic rise in cathodic current at -1.6 volt versus SCE which is of interest.
4. Extrapolation of the linear portion of the cathodic polarization curves to the mixed or rest potential gives the rate of corrosion, the electrochemical estimate agreeing with the rate determined by weight-loss or chemical analyses.
5. A characteristic potential is observed on anodic polarization in halide-containing solutions. This potential is associated with the onset of pitting and may be related to the standard potential for formation of the aluminum halide. Above this critical potential, the current reaches a maximum value which remains constant over a broad potential range.
6. The effect of oxide film thickness on the polarization characteristics depends on whether the electrode reaches equilibrium with the solution before measurements are made.



7. The mixed potential theory can be used to interpret the electrochemical behavior of aluminum. However, the theoretical relation between the mixed potential and the standard electrode potentials of the reactions occurring at the surface needs to be confirmed quantitatively.

The bulk of the available data has thus been obtained in deaerated solutions in the acid range. Limited polarization data are available in strongly alkaline solutions. The near-neutral range, pH 4-8, has been somewhat neglected and the effect of oxygen has not been studied in great detail. Hence, this study of the effect of dissolved oxygen on the polarization characteristics of aluminum in near-neutral solutions appears warranted.

#### Corrosion Behavior of Aluminum

Summaries of the corrosion and oxidation behavior of aluminum are available. (20, (24) The stress-corrosion cracking of some of the high-strength aluminum alloys has also been studied. (3) This discussion is limited to a review of the influence of dissolved oxygen and oxide-film thickness on the rate and nature of corrosion of aluminum in aqueous solutions. The studies described here utilized techniques other than electrochemical; i.e., the criteria for corrosion included determination of weight-losses and pitting penetration rates.

The corrosion of commercially pure aluminum was studied by weight-loss measurements in 0.0001N to 1N potassium chloride solutions at constant temperature. (25) The oxygen concentration was

varied by either bubbling the gas through the solution or by increasing the partial pressure above the solution. The weight-loss of the commercially pure aluminum increased with time and increasing oxygen concentration, and decreased with increasing electrolyte concentration. A direct comparison of the weight-loss at 150 psi in the presence and absence of oxygen established a greater weight-loss in the presence of oxygen. The weight-loss in the presence of oxygen approached a limiting value after about 80 hours, whereas the weight-loss in the absence of oxygen increased linearly with time for about 140 hours. However, when high-purity aluminum (99.99%) was used, the weight-loss was almost zero under similar conditions even when the partial pressure of oxygen was raised to 300 psi. This is additional evidence that the purity of the aluminum is an important factor in determining the effectiveness of dissolved oxygen.

There is convincing evidence that aluminum alloys suffer greater attack in the deep ocean (2370 feet) where the oxygen concentration is low as opposed to surface exposures where the oxygen concentration approaches saturation. Ailor's report of the evaluation of aluminum after one-year deep exposure in the sea showed that high-purity aluminum and alloy 3003 had considerably deeper pitting and higher corrosion rates at the deep-sea location. (26) Reinhart's observations on similar experiments indicated that all the aluminum alloys exhibited more severe pitting and crevice corrosion at depth than near the surface. (27) On the other hand, laboratory studies concerned with the behavior of aluminum in seawater

strongly indicate that elimination of dissolved oxygen from the electrolyte suppresses the corrosion of aluminum alloys 5052, 5454, 6061, and 6063. <sup>(28)</sup> These results strongly suggest that the effectiveness of oxygen depends on composition, but there remain contradictions which are not easily resolved.

The effect of oxide-film thickness on the rate of corrosion of aluminum does not appear to have been studied except by the electrochemical techniques already described. However, there exists a great deal of pertinent work concerned with the chemical, physical and mechanical properties of the aluminum oxide film. The studies of Troutner, <sup>(29)</sup> Hunter and Fowle, <sup>(30)</sup> Dignam, <sup>(31)</sup> Dillon, <sup>(32)</sup> Heine and Pryor, <sup>(33)</sup> and Vermilyea <sup>(34)</sup> are of interest.

## CHAPTER IV

### EXPERIMENTAL DETAILS

The experimental work involved determination of the variation of corrosion potential with pH and measurement of cathodic and anodic polarization data. In addition, controlled-potential weight-loss data were obtained. The materials used, methods of specimen preparation, and the experimental procedures are described below.

#### Materials and Specimen Preparation

High-purity aluminum produced by the Hoopes process, an electrolytic method of purifying commercial aluminum, was used throughout this study. The material was assayed at greater than 99.99% aluminum. The ingots were machined into cylinders which were sectioned into individual specimens having a diameter of 1.9 cm and a thickness of 0.9 cm. Aluminum rod was produced by extrusion of the high-purity material and was used to fabricate the specimen holders which screwed into the specimens.

Preliminary study of methods of preparing the surfaces of the aluminum specimens indicated that pitting during preparation could be minimized by eliminating grinding. As a result, the specimens were polished on a series of cloth wheels following conventional metallographic procedures. The final step in the polishing procedure consisted of electropolishing in a solution containing 104 ml of perchloric acid and 196 ml of acetic anhydride maintained

at less than 13°C at all times to minimize the danger of explosion. The electropolishing bath was operated at 10 a/ft<sup>2</sup>. The specimens were polished for 10 minutes after which they were rinsed in water and methanol and stored in desiccators. Small batches of specimens were prepared weekly. This procedure resulted in specimens with flat mirror-bright surfaces. The specimens were not completely pit-free, however.

The electropolishing solution was chosen so that the thickness of oxide on the surface would be known. The oxide thickness is believed to be in the range of 25-50 angstroms.<sup>(36)</sup> Recent work has shown that constituents of the electropolishing solution may be incorporated in the oxide.<sup>(37)</sup> This may be partially responsible for some of the hysteresis effects described below.

Reagent grade chemicals were used without further purification. Solutions were prepared from water that was first demineralized and then distilled from an alkaline permanganate solution. Solution pH was adjusted with dilute hydrochloric acid or dilute sodium hydroxide. The systems studied were considered to be of sufficient purity to establish the general electrochemical behavior of aluminum and to determine the relative importance of pH, electrode potential and the presence or absence of dissolved oxygen. The degree of purity needed to establish precise values of the electrochemical parameters, in particular Tafel slopes, has not been determined, since it was not the intent of this work to utilize the values as mechanistic indicators. However, impurities present at a level less than 10<sup>-6</sup>M are said to have little effect on the aluminum-water reaction.<sup>(34)</sup>

The most important factor in obtaining reproducible data appears to be control of the thickness and properties of the oxide film always present on aluminum. This is believed to have been accomplished by electropolishing judging from the fact that corrosion potentials became steady quickly. The corrosion potential values were reproducible and were comparable to existing data.

#### Corrosion Potential Measurements

The corrosion potentials were measured as a function of pH using a saturated calomel electrode as the reference electrode and a vacuum tube voltmeter to measure the potential. The measurements were made in 0.5N sodium chloride, in 0.056N sodium sulfate, and in a solution containing 0.5N sodium chloride and 0.056N sodium sulfate. These concentrations correspond to the levels of these salts in seawater. Most of the corrosion potential measurements were made in air-saturated solutions at room temperature (26-28°C). Data were also obtained at pH 4.0 in deoxygenated sodium chloride solutions at 30°C using the polarization cell described below. The specimens were freshly electropolished high-purity aluminum in one series of tests; in a second series of tests, the freshly electropolished high-purity aluminum specimens were etched in 20% hydrofluoric acid for 20 seconds prior to determining the corrosion potential. All the data were obtained in duplicate.

The aluminum specimen and rod were immersed in 500 ml of the test solution along with the reference electrode. The pH of the solution was adjusted at some value between 0 and 14. In the preliminary work, the changes in corrosion potential and pH were

recorded over a 24 hour period. Changes in pH became significant, i.e., greater than 0.1 of a pH unit, after the first hour so that only the initial values and the values after one hour are reported. There was a tendency for the initial pH values to increase with time when the test solution was acidic, and to decrease when the pH of the test solution was between 8 and 11. The measurements were repeated with new specimens and new solutions until the shape of the curve was fairly well-defined over the pH range 0 to 14.

#### Potentiostatic Polarization Measurements

Cathodic and anodic polarization data were obtained at pH 4.0 and at 30°C in air-saturated and deoxygenated 0.5N sodium chloride. A Wenking potentiostat with a range of two volts and a current capacity of 10 amperes was used to control the potential of the electrode within one millivolt. The current was automatically recorded using a Varian instrument having a full scale response time of one second.

The polarization cell was a two-compartment cell connected by a solution bridge. A schematic diagram of the experimental set-up is shown in Figure 6. The large compartment fabricated of polyethylene contained the aluminum specimen and held about 1800 ml of test solution; the other compartment containing the platinum gauze control electrode held about 200 ml of solution. The entire apparatus was placed in a constant temperature water bath which controlled the temperature within 0.1 degree. Provision was made for bubbling air through the solution, or pre-purified nitrogen as

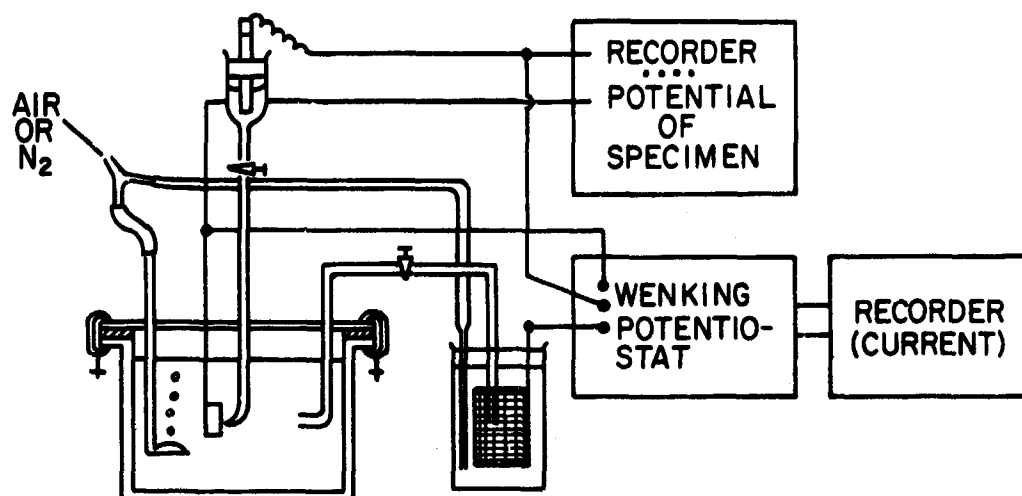


FIGURE 6 SCHEMATIC DIAGRAM OF EXPERIMENTAL SET-UP



required for deoxygenation. The aluminum specimens and holders were coated with Microshield, a stopoff lacquer used in electroplating operations; hence, a known area ( $2.8 \text{ cm}^2$ ) was exposed to the solution.

The specimen was placed in the cell while the appropriate gas was bubbled through the solution. When air was circulated through the cell, little change in the corrosion potential was observed; hence air was circulated for 15 minutes and the corrosion potential recorded for an additional 45 minutes before altering the potential. When nitrogen was bubbled through the system, the corrosion potential became more active, the major change occurring in the first 45 minutes. Hence nitrogen was bubbled through the solution for 60 minutes. The nitrogen inlet tube was then raised to allow nitrogen to flood the space above the solution and to retard ingress of air.

The electrode potential was changed in steps of 20 millivolts, the rate of change being determined by the variation of current with time as observed on the recorder tracings. Current readings became steady within ten minutes over the potential range -0.8 volt to -1.5 volts versus SCE. Beyond this range, the currents became steady within several hours. Hence, the electrode potential was changed when the current became steady except for some of the measurements made in the presence of oxygen.

### Controlled-Potential Weight-Loss Experiments

The controlled-potential weight-loss experiments were conducted in the cell used in the polarization studies. The determinations were made in 0.5N air-saturated sodium chloride at 30°C and at an initial pH of 4.0. The electropolished high-purity aluminum specimen was rinsed in distilled water, methanol and dried for half an hour at 170°C. The specimens were cooled in a desiccator and then weighed. The specimen was heated for an additional ten minutes and then reweighed. The specimen was coated with the stop-off lacquer and when dry, was placed in the cell. When the corrosion potential became steady, a potential was applied by means of the potentiostat. The duration of the tests varied from 24 to 68 hours during which time the current flowing through the cell was measured.

After the test, the lacquer was peeled from the specimen. After rinsing in water and methanol, the specimen was dried for half an hour at 170°C, cooled and weighed. The specimen was reweighed after an additional ten minutes in the oven to make sure the specimen was thoroughly dried. In general, the two successive weight determinations agreed within 0.0002 grams. The specimen was then placed in the stripping solution, containing 450 g of chromic acid and 475 ml of phosphoric acid and operated at 92°C, for ten minutes, rinsed in water and methanol, dried as above and reweighed until there was agreement between successive readings. An uncorroded specimen lost less than 0.0005 gram during the above treatments. The pH of the solution was measured at the end of each test.

## CHAPTER V

### RESULTS AND DISCUSSION

The variation of the corrosion potential of aluminum with pH has been determined. Cathodic and anodic polarization data, as well as controlled-potential weight-loss data, were obtained in solutions of sodium chloride at pH 4.0. The analysis of the data is based on the behavior characteristic of metals displaying stable passivity, and on the concept of the mixed potential. This interpretation makes it possible to construct a corrosion diagram which is consistent with the observed variation of corrosion potential with pH and which leads to estimates of the rate of dissolution of aluminum as a function of pH.

#### Corrosion Potentials of High-Purity Aluminum

The corrosion potential of the electropolished high-purity aluminum was measured at pH 4.0 in 0.5N sodium chloride at 30°C in the presence and absence of dissolved oxygen. The average value of the corrosion potential in the presence of oxygen was  $-1.239 \pm 0.030$  volts versus the saturated calomel electrode (SCE); in the absence of oxygen, the value was  $-1.308 \pm 0.006$  volts versus SCE. The values are those measured at the end of one hour and are based on a minimum of six determinations. Hence, the presence of oxygen caused a shift in the corrosion potential of about 70 millivolts which, in contrast to the behavior of nickel, appears relatively small. (6)

Because the corrosion potential of high-purity aluminum was only slightly affected by the presence of oxygen at pH 4.0, the measurements of the corrosion potential at other values of the pH were conducted in air-saturated solutions. The results for the electropolished high-purity aluminum are given in Figures 7, 8, and 9. Included in the figures are data obtained immediately on immersion of the specimen in the given solution and the data after one hour.

The variation in the corrosion potential with pH is similar in each of the three solutions tested. The corrosion potential decreases as the pH is increased in the range 0 to 4 and 8 to 14. In the intermediate range (4-8), the potential increases with pH.

The results using electropolished specimens which were etched in dilute hydrofluoric acid before determining the corrosion potential are given in Figures 10, 11, and 12. Although the variation of the corrosion potential with pH is not as smooth as that observed with electropolished high-purity aluminum, the variation appears linear at low and high pH. The tendency for the corrosion potential to increase with increasing pH in the range 4 to 8 is still evident.

The degree and extent of the corrosion observed on the high-purity aluminum specimens used in determining the corrosion potentials varied with pH. Slight pitting and some etching of the specimens occurred below pH 4.0. In the intermediate range (pH 4.0 to 8.0), pitting was the predominant mode of attack. Above pH 8.0 and especially at pH 10.0, there was a tendency for the specimen to tarnish as well as to pit. The film which formed at pH 10 appeared

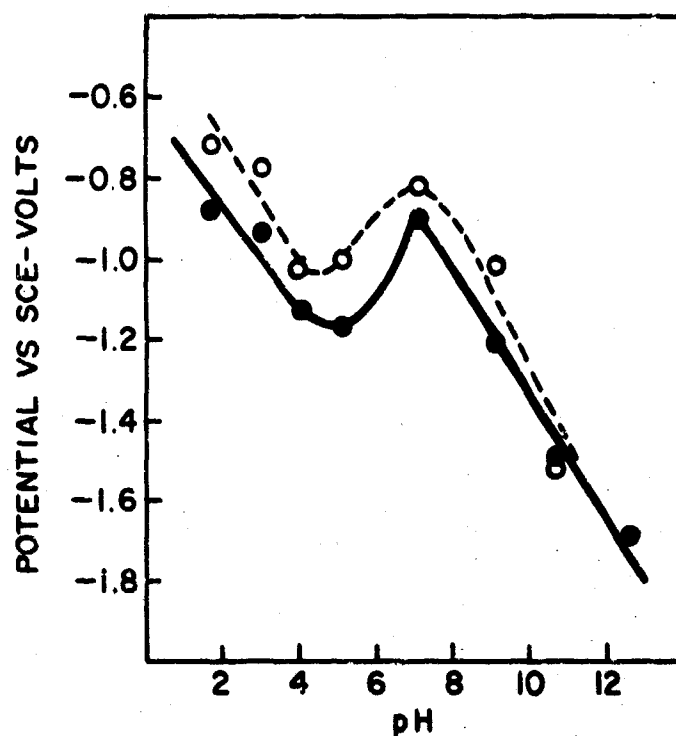
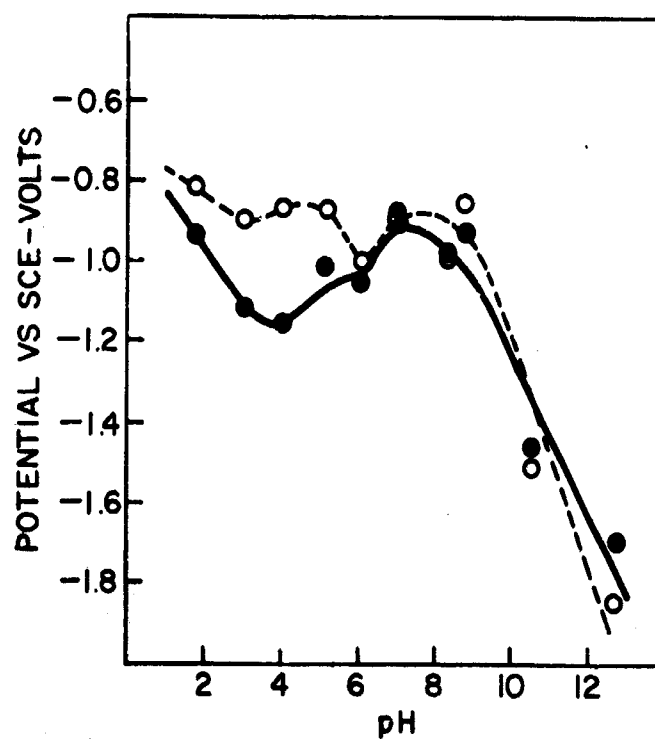


FIGURE 7 CORROSION POTENTIALS OF ELECTROPOLISHED HIGH-PURITY ALUMINUM AS A FUNCTION OF pH IN AIR-SATURATED 0.056N SODIUM SULFATE AT ROOM TEMPERATURE: O INITIAL VALUES; ● ONE HOUR VALUES



**FIGURE 8** CORROSION POTENTIALS OF ELECTROPOLISHED HIGH-PURITY ALUMINUM AS A FUNCTION OF pH IN AIR-SATURATED 0.5N SODIUM CHLORIDE AT ROOM TEMPERATURE: O INITIAL VALUES; ● ONE HOUR VALUES

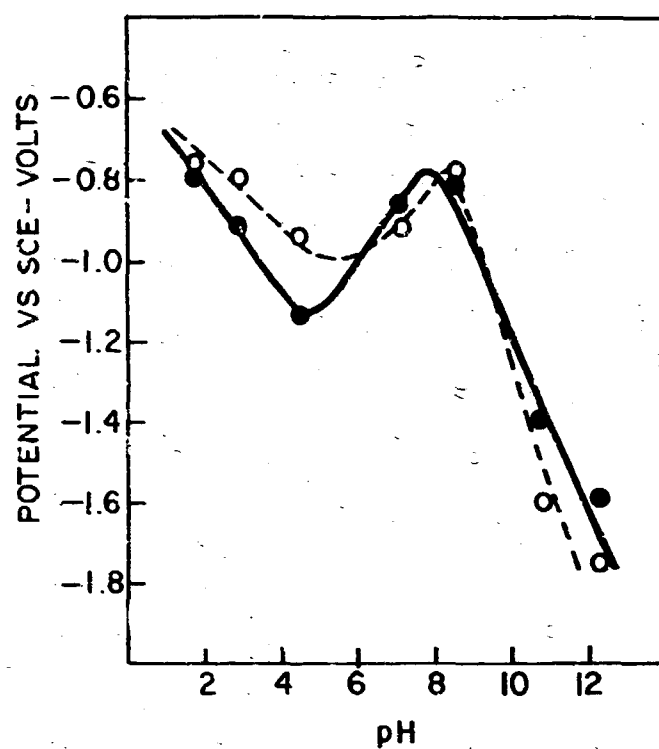


FIGURE 1. CORROSION POTENTIALS OF ELECTROPOLISHED HIGH-PURITY ALUMINUM AS A FUNCTION OF pH IN AIR-SATURATED 0.5N SODIUM CHLORIDE AND 0.056N SODIUM SULFATE AT ROOM TEMPERATURE: O INITIAL VALUES, ● ONE HOUR VALUES

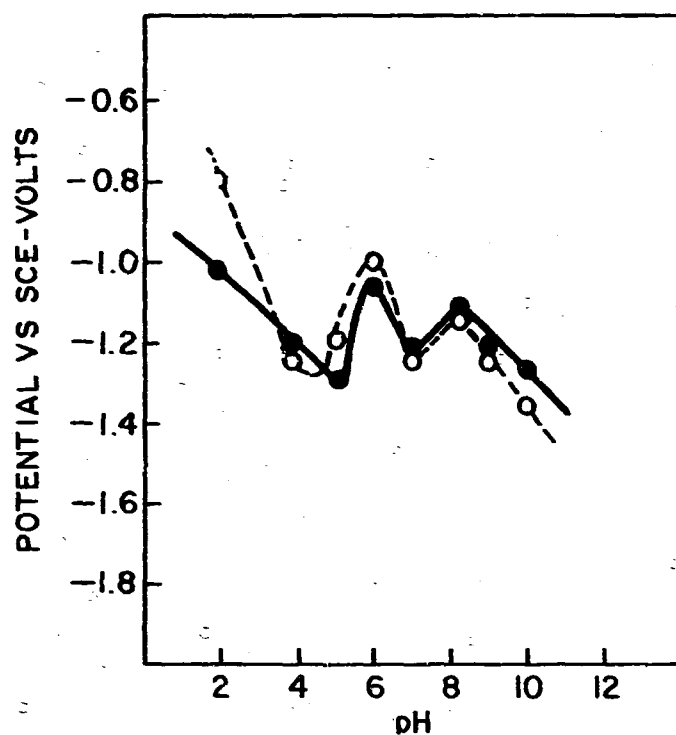


FIGURE 10 CORROSION POTENTIALS OF ETCHED HIGH-PURITY ALUMINUM AS A FUNCTION OF pH IN AIR-SATURATED 0.5N SODIUM CHLORIDE AT ROOM TEMPERATURE: ○ INITIAL VALUES, ● ONE HOUR VALUES



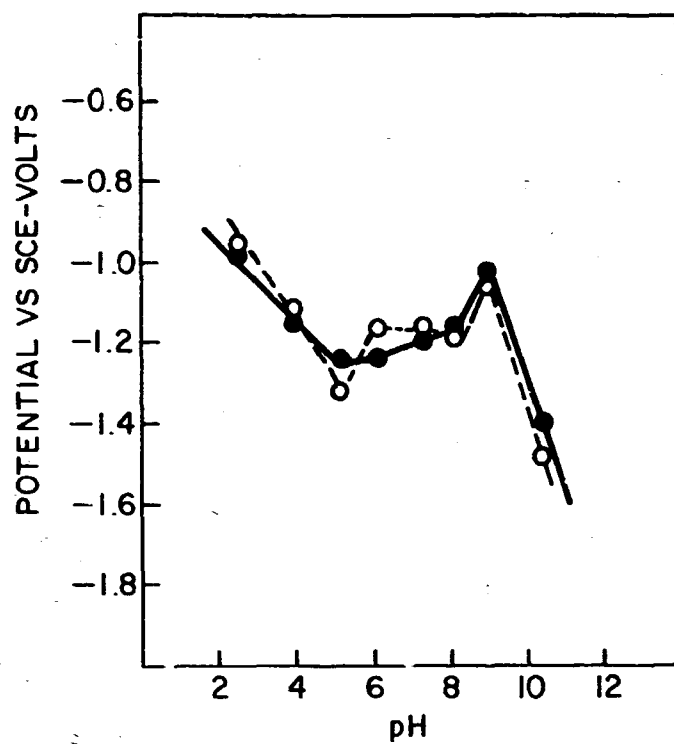


FIGURE 11 CORROSION POTENTIALS OF ETCHED HIGH-PURITY ALUMINUM AS A FUNCTION OF pH IN AIR-SATURATED 0.056N SODIUM SULFATE AT ROOM TEMPERATURE: O INITIAL VALUES, ● ONE HOUR VALUES

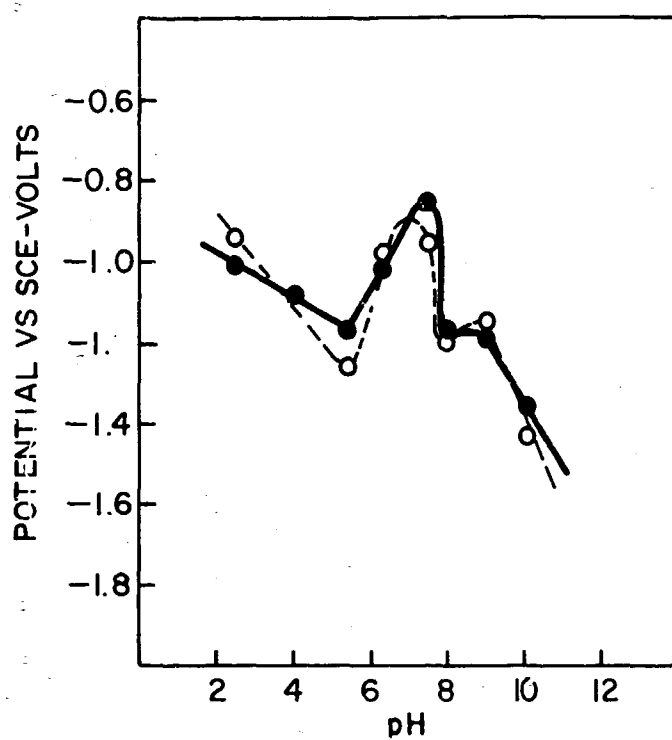


FIGURE 12 CORROSION POTENTIALS OF ETCHED HIGH-PURITY ALUMINUM AS A FUNCTION OF pH IN AIR-SATURATED 0.5N SODIUM CHLORIDE AND 0.056N SODIUM SULFATE AT ROOM TEMPERATURE: ○ INITIAL VALUES, ● ONE HOUR VALUES

dark, but displayed a wide range of colors under the microscope, the colors varying from yellow to red to blue at the perimeter of the pits.

The evolution of hydrogen was difficult to detect in the acid range, occurred slowly above pH 8.0, and vigorously above pH 12.0. A precipitate of aluminum hydroxide formed rapidly above pH 12.0 and the specimens were etched deeply.

The above results indicate that the mixed or corrosion potential of high-purity aluminum is only slightly affected by the presence of oxygen, but is sensitive to the variations in pH of the test solution. The initial corrosion potential values are not especially sensitive to the anions present in solution, although the corrosion potentials in the absence of chloride were generally noble to the values determined in sodium chloride. Although the data used to construct the corrosion potential--pH curves are values obtained after one hour, the overall shape of the curves is similar to a curve obtained by Haynie and Ketcham in 0.2N NaCl.<sup>(11)</sup> The linear variation at low and high pH and the ennoblement of the corrosion potentials in the intermediate pH range are, therefore, believed to be characteristic of the electrochemical behavior of oxide-covered aluminum. The significance of the corrosion potential--pH curve will be discussed after presenting the results of the cathodic and anodic polarization studies conducted at pH 4.0.

### Polarization Behavior at pH 4.0

Figure 13 shows the results of cathodic polarization of freshly electropolished high-purity aluminum in deaerated 0.5N sodium chloride at pH 4.0. Two sets of data are included in the figure to emphasize the reproducible nature of the curves. The current-voltage curves are characterized by linear sections at low and high current densities having slopes of -0.140 and -0.120, respectively. The current density is constant in the range -1.46 to -1.60 volts versus SCE. There is a tendency for the current density to decrease as the potential approaches -1.6 volts, but this was not always observed, as indicated by the data in the figure.

Figure 14 gives the results of cathodic polarization of freshly electropolished high-purity aluminum in air-saturated 0.5N sodium chloride. Included in Figure 14 is one of the curves obtained in deaerated sodium chloride. The presence of oxygen shifts the curves in the noble direction and increases the cathodic current density at a given electrode potential; for example, at -1.4 volts, the average current density increases from  $5.3 \pm 0.6 \mu\text{A}/\text{cm}^2$  in deaerated sodium chloride to  $7.8 \pm 1 \mu\text{A}/\text{cm}^2$  in the air-saturated solution. The constant current region observed in the deaerated sodium chloride is not well-defined in the presence of oxygen; however, the inflection in the curves obtained in air-saturated solutions occurs at about the same current density at which the constant current region was observed in the deaerated solution, suggesting that a characteristic change in the electrode process

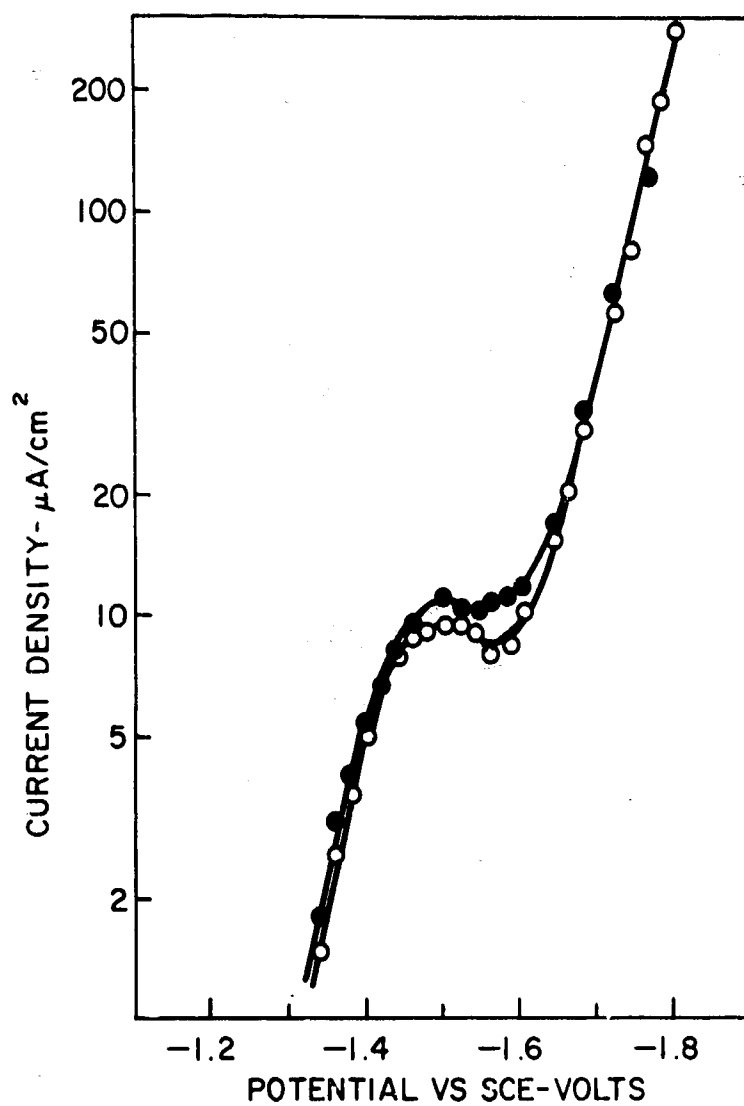


FIGURE 13 DUPLICATE RESULTS OF CATHODIC POLARIZATION OF ELECTROPOLISHED HIGH-PURITY ALUMINUM IN DEAERATED 0.5N SODIUM CHLORIDE AT 30°C AND pH 4.0

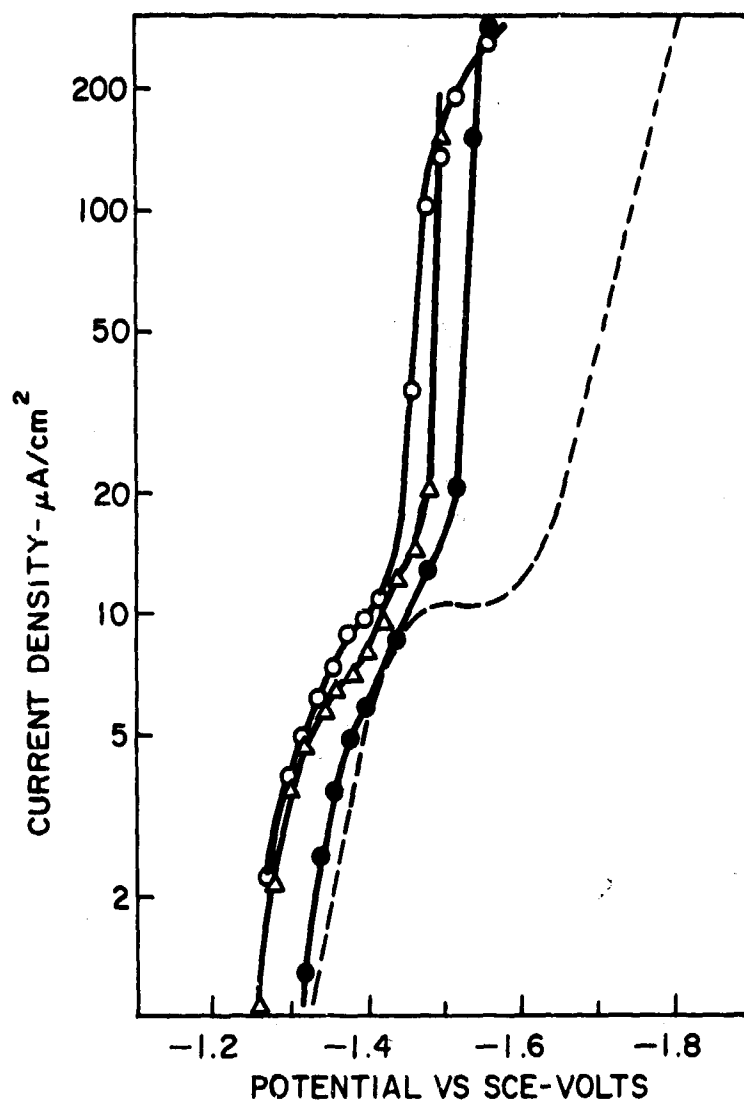


FIGURE 14 TRIPLICATE RESULTS OF CATHODIC POLARIZATION OF ELECTROPOLISHED HIGH-PURITY ALUMINUM IN AIR-SATURATED 0.5N SODIUM CHLORIDE AT 30°C AND pH 4.0, INCLUDING A RESULT IN THE ABSENCE OF OXYGEN (DOTTED LINE)

occurs at about  $10 \mu\text{A}/\text{cm}^2$ . A rapid rise in current occurs at -1.5 volts with oxygen present in solution. The currents continue to increase for long periods of time and in some instances fail to attain steady values. An increased tendency for the aluminum to pit in the air-saturated solution was also observed. Pit propagation is probably the cause of the difficulty in establishing a linear relation at high current density in air-saturated solutions. Evidence for this is provided below. Little pitting of the specimens was detected after cathodic polarization in deaerated sodium chloride.

The data in Figures 13 and 14 are characteristic of freshly electropolished high-purity aluminum exposed to the test solution about an hour prior to commencing cathodic polarization. Figure 15 shows the results of cathodic polarization of high-purity aluminum in air-saturated sodium chloride, the specimen being electropolished, etched in dilute hydrofluoric acid and exposed to the solution 24 hours prior to obtaining the data. The corrosion potential was -1.25 volts versus SCE after about an hour, in agreement with other determinations, and after 24 hours it increased to -0.86 volts. The polarization curve in air-saturated solution has a linear region at low current density with a slope of -0.28 volts and a constant current region extending from -1.2 to -1.4 volts, the current density varying from 6 to  $7 \mu\text{A}/\text{cm}^2$ . There is a suggestion that a second current density plateau commences at -1.3 volts and this may correspond to the reduction of oxygen. If so, the reduction of oxygen contributes about  $1 \mu\text{A}/\text{cm}^2$  to the net cathodic limiting current density. A

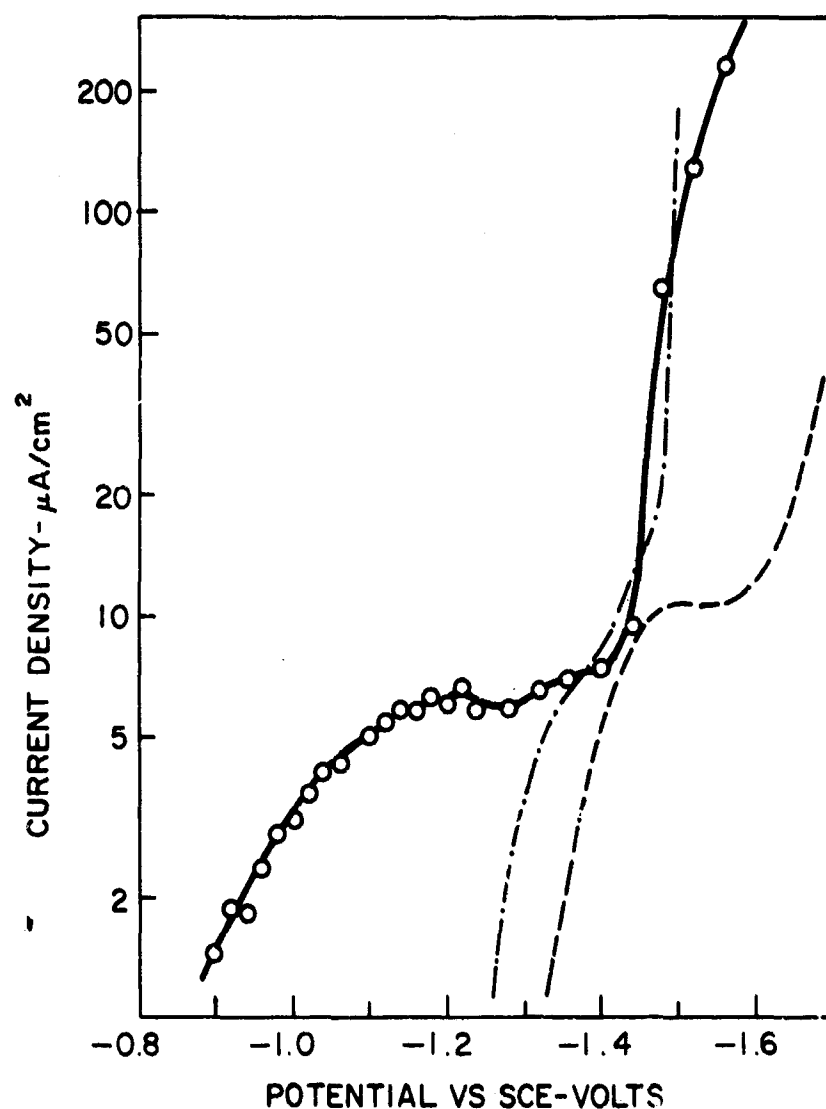


FIGURE 15 CATHODIC POLARIZATION OF HIGH-PURITY ALUMINUM IN 0.5N SODIUM CHLORIDE AT 30°C AND pH 4.0: O AFTER 24 HOURS EQUILIBRATION IN THE PRESENCE OF OXYGEN, -.-. AFTER 1 HOUR EQUILIBRATION IN THE PRESENCE OF OXYGEN; --- AFTER 1 HOUR EQUILIBRATION IN THE ABSENCE OF OXYGEN



rapid rise in current occurs at -1.48 volts in good agreement with the other measurements made in air-saturated solutions.

That the rapid increase of current density in the presence of oxygen and the failure to establish a linear relation above  $10 \mu\text{A}/\text{cm}^2$  is due to pitting of the specimens is supported by the data given in Figure 16. The specimen used to obtain the data (open circles) in Figure 16 was electropolished, immersed in 1:1 nitric acid for 5 seconds, and thoroughly rinsed before obtaining the cathodic polarization data. The results obtained with the nitric acid-treated specimen are in good agreement at low current density with those obtained using freshly electropolished aluminum in air-saturated solutions, but show a distinct constant current density region, and a linear section above  $10 \mu\text{A}/\text{cm}^2$ . The slope of the current-voltage curve above  $10 \mu\text{A}/\text{cm}^2$  is -0.160. Considerably less pitting occurred during cathodic polarization of the nitric acid-treated specimen than with freshly electropolished aluminum in air-saturated sodium chloride.

Figures 17 and 18 give two examples of hysteresis effects observed during cathodic polarization of high-purity aluminum. Figure 17 shows the effect of repeated cathodic polarization in deaerated sodium chloride. After the first set of data were obtained, the circuit was opened and the specimen assumed a corrosion potential of -1.3 volts rather quickly. The cathodic polarization was then repeated and with the exception of the lower limiting current density, the two sets of data are comparable. Figure 18 shows an attempt to retrace the cathodic polarization curve in air-saturated sodium chloride without opening the circuit; the specimen was

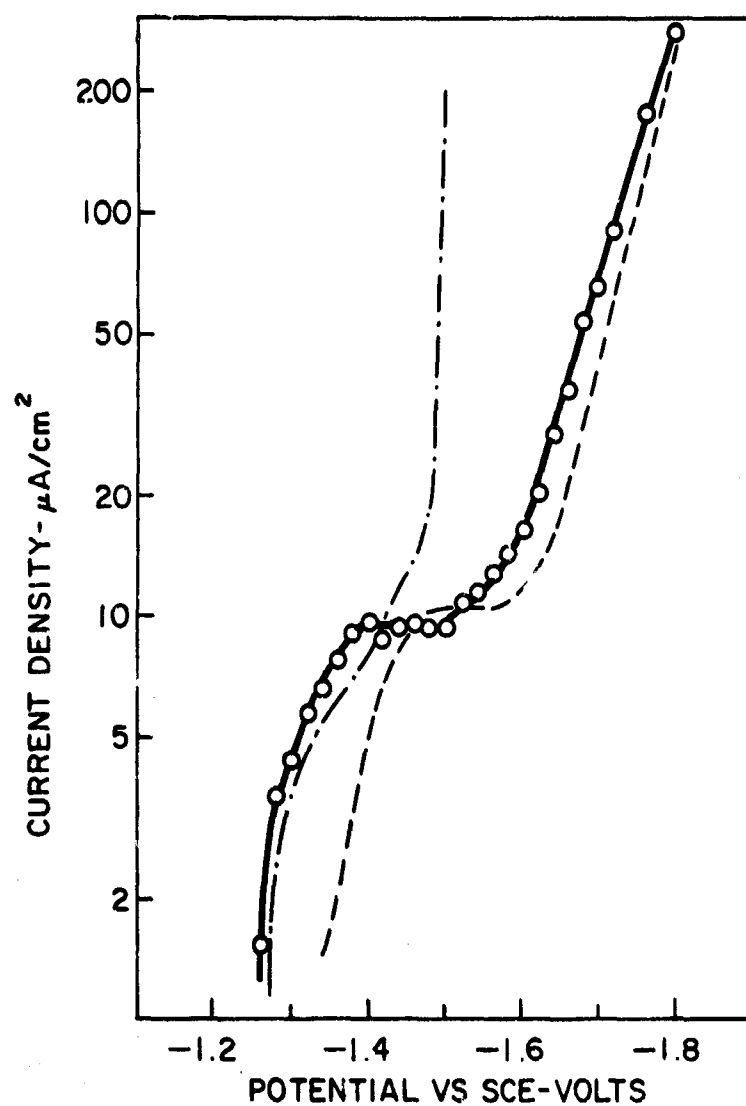


FIGURE 16 CATHODIC POLARIZATION OF HIGH-PURITY ALUMINUM IN AIR-SATURATED 0.5N SODIUM CHLORIDE AT 30°C and pH 4.0:  
 O NITRIC ACID-TREATED SPECIMEN; ---. ELECTROPOLISHED AND POLARIZED IN THE PRESENCE OF OXYGEN; --- ELECTROPOLISHED AND POLARIZED IN THE ABSENCE OF OXYGEN

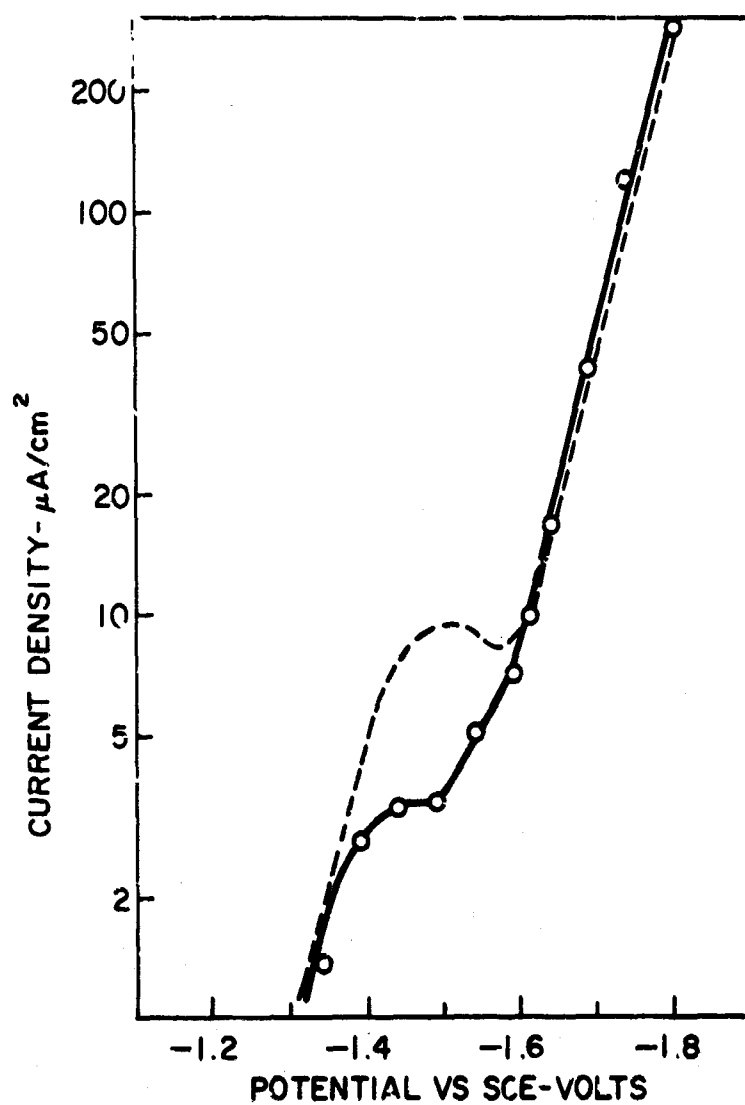
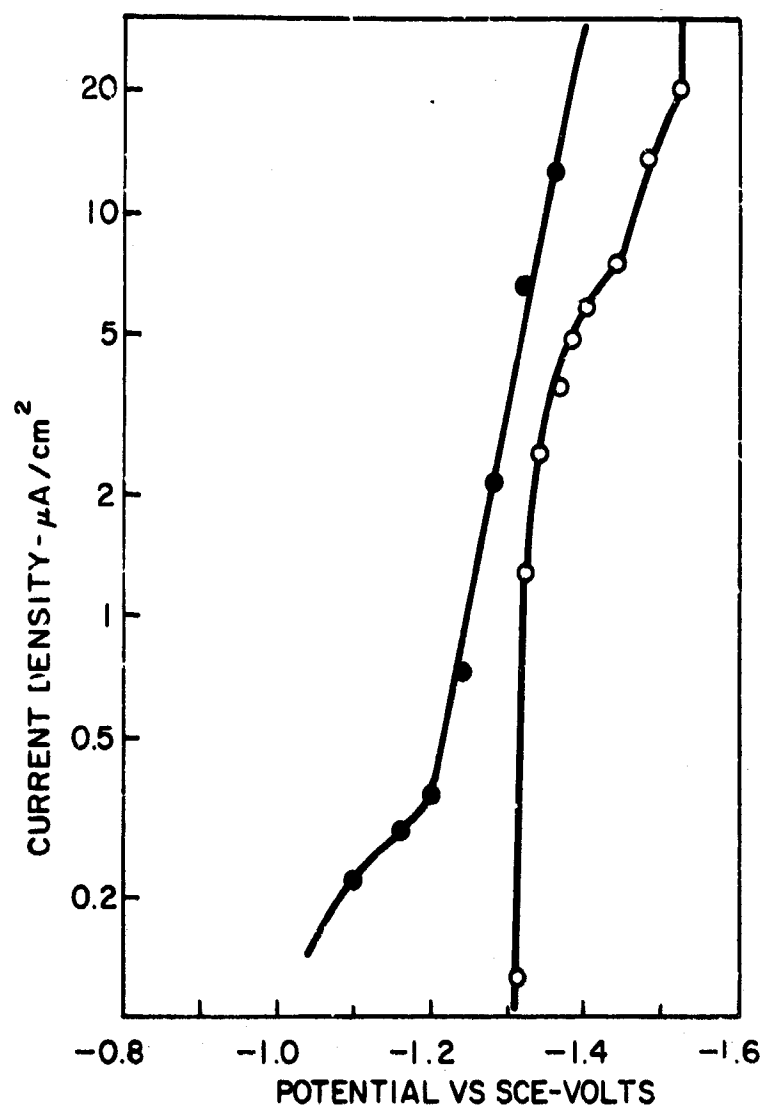


FIGURE 17 CATHODIC POLARIZATION OF HIGH-PURITY ALUMINUM IN DEAERATED 0.5N SODIUM CHLORIDE AT 30°C AND pH 4.0: --- FIRST DETERMINATION, O SECOND DETERMINATION ON SAME SPECIMEN, THE CIRCUIT BEING OPENED BETWEEN DETERMINATIONS



**FIGURE 18 CATHODIC POLARIZATION OF HIGH-PURITY ALUMINUM IN AIR-SATURATED 0.5N SODIUM CHLORIDE AT 30°C AND pH 4.0: ○ FIRST DETERMINATION; ● SECOND DETERMINATION, THE SPECIMEN BEING POLARIZED FROM -1.6 TO -1.12 VOLTS WITHOUT OPENING THE CIRCUIT BETWEEN DETERMINATIONS**

cathodically polarized to -1.6 volts and the applied potential was then increased from -1.6 volts to -1.12 volts in 40 mv steps. The descending branch of the curve is linear with a slope of -0.11 and the inflection in the descending branch of the curve occurs at a low current density.

The anodic polarization data of freshly electropolished high-purity aluminum in air-saturated sodium chloride is given in Figure 19. Included in Figure 19 is a corresponding cathodic polarization curve and a second anodic polarization curve showing the effect of repeated anodic polarization.

A characteristic feature of the anodic curves is the rapid rise in current at -0.74 volts, termed the critical pit initiation potential by other investigators. Above -0.74 volts, the current becomes constant, attaining a value of  $0.6-0.8 \text{ ma/cm}^2$  under the present experimental conditions. Similar results have been reported by others. Although the anodic curve appears to have a linear region at low current density, it appears to approach a limiting value just prior to reaching the critical pitting potential. As with repeated cathodic polarization, the repetition of anodic polarization on the same specimen results in a reduction in the rate of the electrode process.

Figure 20 shows cathodic and anodic polarization curves obtained in deaerated sodium chloride on repeated polarization. The anodic curve appears to be approaching a limiting value of about  $2 \text{ } \mu\text{A/cm}^2$  in the absence of oxygen and the comparable curve

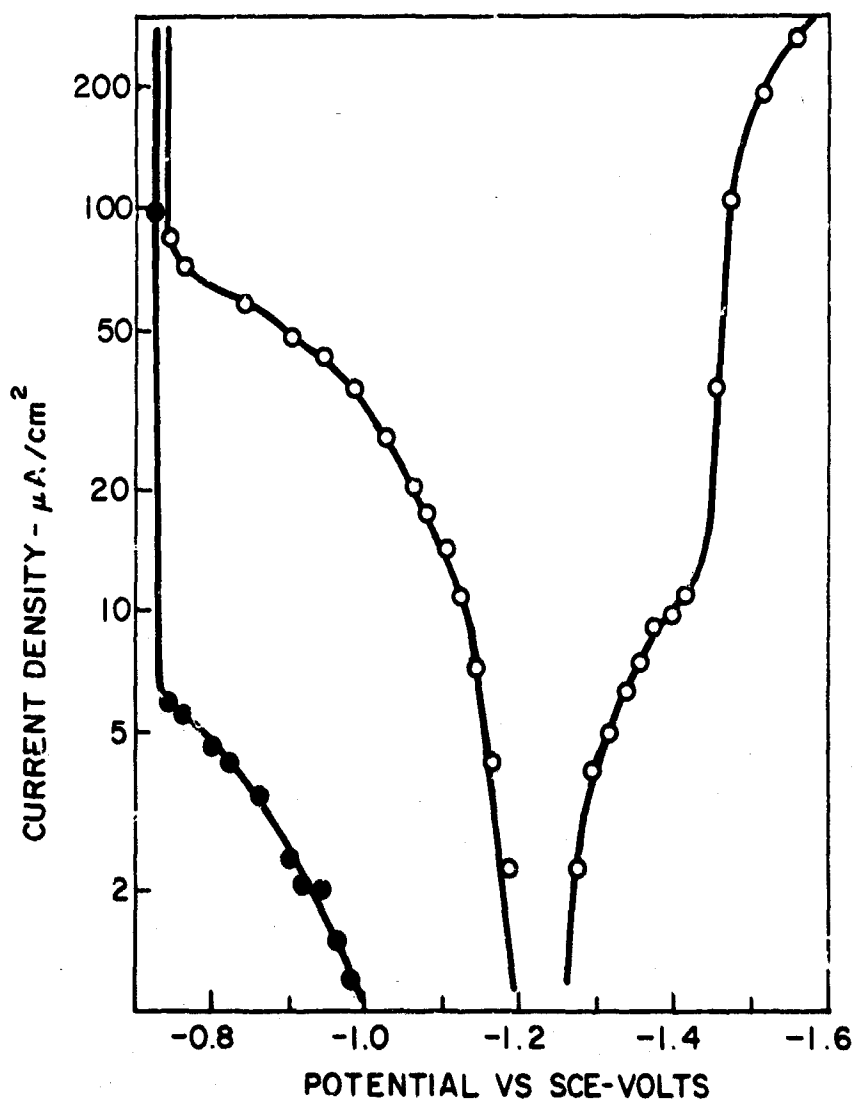


**FIGURE 19 CATHODIC AND ANODIC POLARIZATION OF HIGH-PURITY ALUMINUM IN AIR-SATURATED 0.5N SODIUM CHLORIDE AT 30°C AND pH 4.0:  
○ FIRST DETERMINATION OF CATHODIC AND ANODIC POLARIZATION;  
● SECOND DETERMINATION ON SAME SPECIMEN, THE CIRCUIT BEING OPENED BETWEEN DETERMINATIONS**

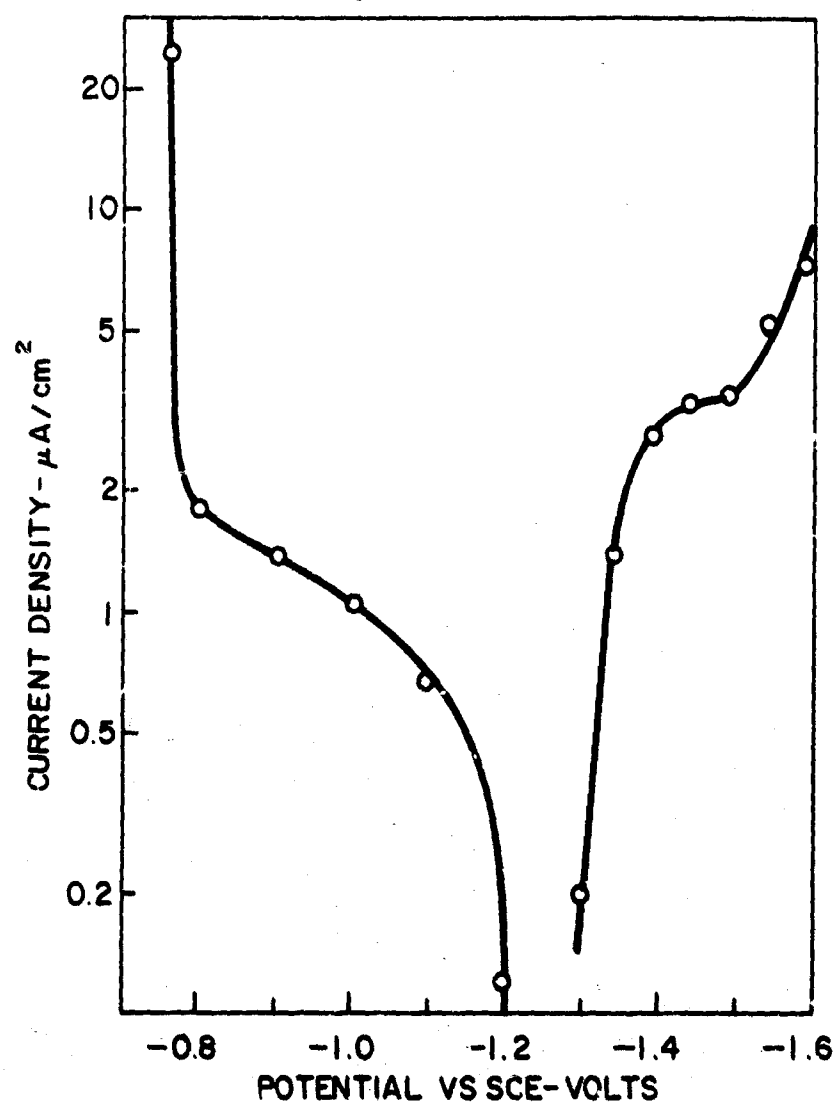


FIGURE 20 EFFECT OF REPEATED CATHODIC AND ANODIC POLARIZATION OF HIGH-PURITY ALUMINUM IN DEAERATED 0.5N SODIUM CHLORIDE AT 30°C AND pH 4.0

in Figure 19 (closed circles) approaches a limiting value of about  $6 \mu\text{A}/\text{cm}^2$  in the presence of oxygen. Oxygen thus appears to have a small influence on the rate of the anodic process.

#### Controlled-Potential Weight-Loss Data

Weight-loss data were obtained as a function of the electrode potential to aid in the interpretation of the polarization data. Since weight-loss data can be expressed in terms of current density, controlled-potential weight-loss data can be used to construct "anodic polarization curves". An anodic polarization curve based on weight-loss data should correspond to the anodic self-polarization curve ( $i_a$  in Figure 4(A)). The curves given in Figures 13 to 20 correspond to the net current density ( $I$  in Figure 4(B)). Knowing  $I$  and  $i_a$ , it should be possible to calculate the cathodic self-polarization data,  $i_c$ , and construct corrosion diagrams already described (Figures 3, 4(A)). This is feasible when two simultaneous processes are taking place at the electrode surface and one is over-all cathodic and the other is over-all anodic, e.g., the situation depicted in Figure 3.

The rate of corrosion of high-purity aluminum is low and very sensitive to changes in pH of the electrolyte. Precise values of the rate of corrosion of aluminum are difficult to determine by measuring the loss in weight of specimens in simple beaker-type experiments. The values given below should therefore be considered estimates of the order of magnitude of the rate of corrosion of freshly electropolished high-purity aluminum.



The controlled-potential weight-loss data are given in Table 1. The initial pH was 4.0 and the final pH of the 0.5N NaCl solution is given in the table. The corrosion potential of the high-purity aluminum is about -1.24 volts versus SCE as already stated. The data thus indicate that aluminum corrodes at potentials both cathodic and anodic to its corrosion potential. Comparison of the two results obtained at -1.5 volts indicates that the important factor is the increasing alkalinity of the environment as the time of the experiment increases. At -0.8 volt the pH change is not as great as at -1.5 volts and the rate of corrosion is less than at the lower potential. The fact that the pH of the solution changes only slightly at -1.3 and -1.4 volts indicates that the rates of the cathodic and anodic processes are virtually in balance and, therefore, the rates of corrosion observed are characteristic of the initial pH of the solution and the electrode potential. The rate of corrosion of freshly electropolished high-purity aluminum appears to be of the order of  $10 \mu\text{A}/\text{cm}^2$  at pH 4.0 in air-saturated 0.5N sodium chloride. Of greater significance, however, is the fact that cathodic and anodic processes occur simultaneously over the entire potential range -0.8 to -1.5 volts encompassing the observed corrosion potentials of aluminum.

The data are plotted in Figure 21 to compare the present results with those of Kunze.<sup>(23)</sup> Similar trends in both sets of data are evident. However, Kunze's data also indicate that the rate of corrosion of aluminum is nearly independent of electrode potential

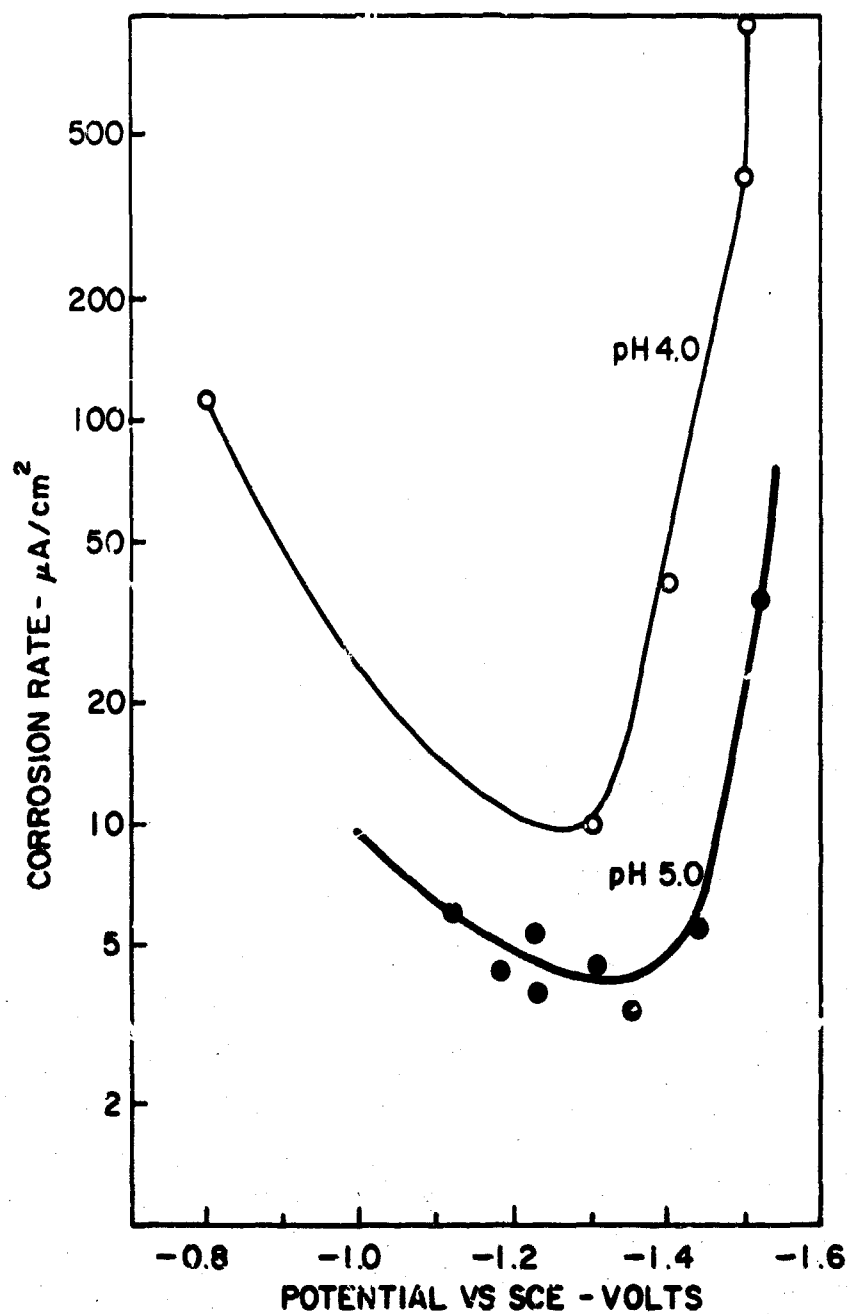


**FIGURE 21 COMPARISON OF CONTROLLED-POTENTIAL WEIGHT-LOSS DATA AT pH 4.0 IN AIR-SATURATED 0.5N SODIUM CHLORIDE WITH RESULTS REPORTED BY KUNZE IN DEAERATED BUFFERED 0.5N SODIUM CHLORIDE AT pH 5.0**

TABLE 1

## SUMMARY OF CONTROLLED-POTENTIAL WEIGHT-LOSS EXPERIMENTS

Run Number	Potential (Volts versus SCE)	Final* pH	Weight Loss (Grams)	Time (Hours)	Corrosion (Rate $\mu\text{A}/\text{cm}^2$ )
1	-1.5	8.6	0.0101	26.5	410
2	-1.5	9.6	0.0415	44.8	990
3	-1.4	4.2	0.0025	67.4	40
4	-1.3	4.1	0.0005	64.0	10
5	-0.8	7.0	0.0026	24.8	113

\*The initial pH was 4.0.

over the range -1.1 to -1.42 volts versus SCE. Data reported by Vermilyea also indicate that the rate of corrosion of aluminum varies only slightly over the potential range -0.5 to -1.6 volts versus SCE in 0.01N ammonium acetate.<sup>(34)</sup> Thus, at constant pH, the anodic self-polarization curve for aluminum can be approximated by a constant current density line extending from about -0.8 to -1.6 volts. This conclusion is of special interest because it suggests that the electrochemical behavior of aluminum is consistent with the behavior of metals that show stable passivity.<sup>(6)</sup>

#### Interpretation of the Results

The analysis of the results is based on the conclusion of the previous section that the electrochemical behavior of aluminum is consistent with the behavior of metals displaying stable passivity. The implications of this are worth examining.

The self-polarization and the experimentally measurable external polarization curves of a metal that exhibits stable passive behavior are drawn schematically in Figure 22. Figure 22(A) illustrates that the mixed or corrosion potential,  $E_m$ , corresponds to the point of intersection of the cathodic and anodic self-polarization curves in the passive region, BCD. Algebraic summation of the curve, ABCD, and the curve, EFG, results in the curve given in Figure 22(B). The latter can be determined experimentally. The usual practice of estimating the rate of corrosion of a metal by extrapolating linear sections of the curve to the corrosion potential will, in this case, give values of the corrosion rate which are

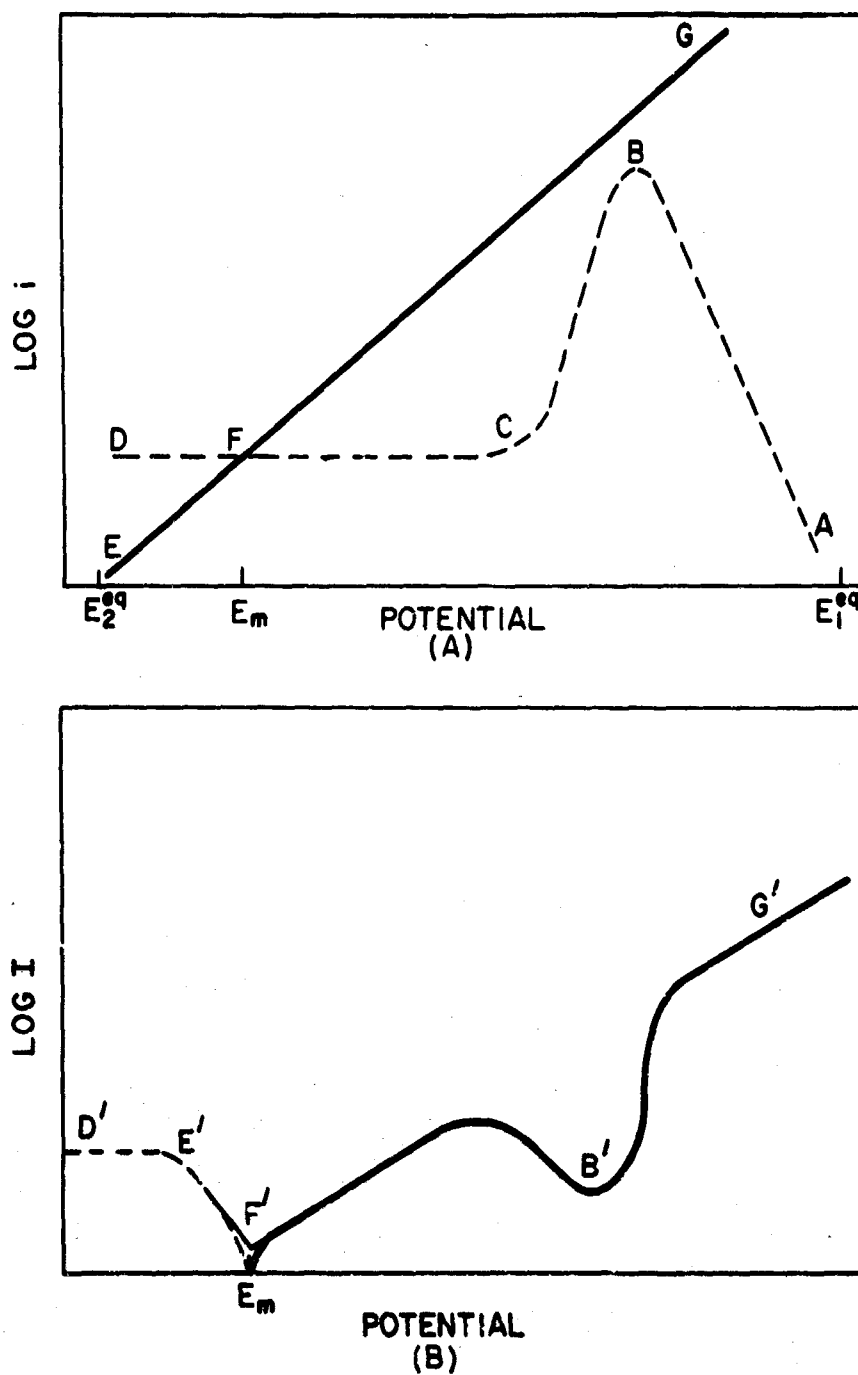


FIGURE 22 POLARIZATION CHARACTERISTICS OF A METAL DISPLAYING STABLE PASSIVE BEHAVIOR: (A) SELF-POLARIZATION CURVES, (B) CORRESPONDING EXTERNAL POLARIZATION CURVES. ANODIC CURRENTS INDICATED BY DOTTED LINES

lower than the actual value. The actual rate of corrosion is given by the constant current density line, CFD, in the self-polarization diagram, Figure 22(A). The anodic portion of the external polarization curve, F'E'D', approaches the actual rate of corrosion as a limiting value. Thus, for a metal displaying stable passive behavior, the experimentally determined anodic polarization curve should approach a limiting value indicative of the rate of corrosion of the metal.

The results of this study indicate that the electrochemical behavior of aluminum is an example of the stable passive behavior of metals. In particular, the results of the controlled-potential weight-loss experiments show that, in order to account for the pH changes observed, cathodic and anodic processes must occur simultaneously over the entire range of potentials studied. This is in accord with the behavior expected from Figure 22(A). In addition, the anodic polarization data appear to approach limiting current density values prior to reaching the characteristic pit initiation potential. Many of the hysteresis effects appear consistent with the presence on the surface of aluminum of a stable oxide film. These observations, coupled with the data of Kunze and Vermilyea which indicate that the rate of corrosion of aluminum is virtually independent of electrode potential over a broad range, support the conclusion that the electrochemical behavior of aluminum is representative of the stable passive state of metals. On this basis, the limiting anodic current density values prior to the point of rapid pit initiation should be used to estimate the rate of corrosion of aluminum.

The experimental data summarized in Figures 13 to 20 have been examined in light of the above analysis. Based on the anodic polarization data given in Figure 19, the rate of corrosion of freshly electropolished high-purity aluminum in air-saturated 0.5N sodium chloride would be  $70 \mu\text{A}/\text{cm}^2$ . This value is believed to be characteristic of freshly electropolished high-purity aluminum exposed to the solution for one hour prior to commencing polarization. Longer times of exposure appear to reduce the initial rate of corrosion of the electropolished aluminum to  $10 \mu\text{A}/\text{cm}^2$  as indicated by the results of the weight-loss experiments.

The self-polarization curves which are consistent with the above estimates of the rate of corrosion of aluminum and with the experimentally determined curves are given in Figure 23. Algebraic summation of the anodic self-polarization curve,  $i_{a, 1}$ , and the cathodic self-polarization curve,  $i_{c, 1}$ , results in curves which are in good agreement with the data given in Figures 13, 14, and 19. The summation of the indicated curves, however, does not reproduce the rapid rise in current observed at -1.5 volts versus SCE in the air-saturated solutions. The effect has been attributed to pitting. Evidence already presented indicates that in the absence of pitting, the experimentally determined curves would coincide in air-saturated and deoxygenated solutions at current densities above  $10 \mu\text{A}/\text{cm}^2$ . Similarly, algebraic summation of curves,  $i_{a, 2}$ , and  $i_{c, 2}$ , in Figure 23 yields the experimentally determined cathodic curve given in Figure 15, with the exception of the rapid rise in current at -1.5 volts versus SCE when oxygen is present.

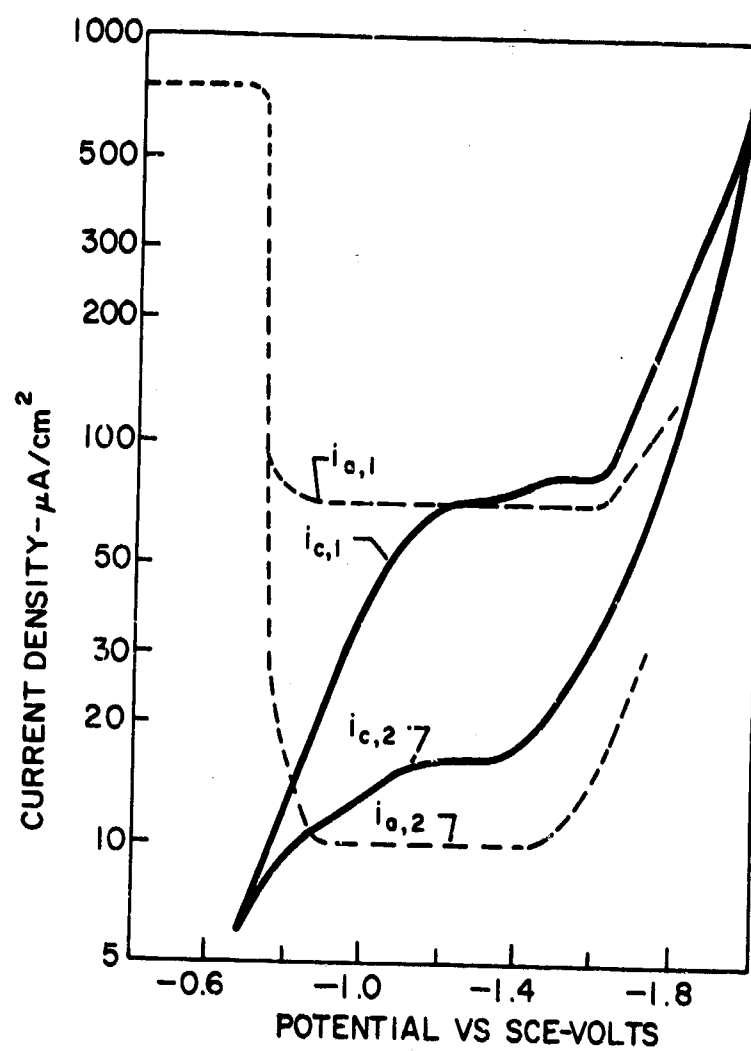


FIGURE 23 SELF-POLARIZATION CURVES OF HIGH-PURITY ALUMINUM IN 0.5N SODIUM CHLORIDE AS CONSTRUCTED FROM THE EXPERIMENTAL DATA



Summation of the curves  $i_{a, 1}$  and  $i_{c, 1}$  in Figure 23 results in almost exact agreement with the experimental results obtained in deaerated solutions; the calculated curve agrees within  $\pm 50$  millivolts with the experimental results obtained in air-saturated solutions. It has, therefore, been implied that the diagram of Figure 23 applies equally well to air-saturated and deoxygenated solutions of sodium chloride. However, better agreement with the experimental data obtained in the presence of oxygen would result by shifting the cathodic self-polarization curve,  $i_{c, 1}$ , in the noble direction, or by shifting the anodic self-polarization curve,  $i_{a, 1}$ , to a somewhat lower current density. It is difficult to decide between these two alternatives on the basis of the available data. In general, however, the effect of dissolved oxygen on the rates of the cathodic and anodic processes taking place at the high-purity aluminum electrode is slight. In this context, the statement by Mears that the corrosion rate of aluminum and its alloys is relatively insensitive to the amounts of oxygen commonly encountered in most practical environments appears reasonable. (38) Implications that the corrosion rate of aluminum in aqueous solutions can be arrested almost completely, or conversely, increased by complete elimination of oxygen do not seem reasonable. (39), (40) The overvoltage for the reduction of oxygen on oxide-covered aluminum must, therefore, be high, and the presence of dissolved oxygen in solution has little influence on the rate of corrosion of high-purity aluminum. The predominant cathodic reaction occurring during corrosion is, by process of elimination,

the reduction of hydrogen ions. Although oxygen may have a greater effect on the corrosion rate of alloys of aluminum, the reduction of hydrogen ions should still predominate.

Dissolved oxygen does, however, increase the tendency for the high-purity aluminum to pit when cathodically polarized. One conclusion that may be drawn is that cathodic protection of aluminum should be more effective in the absence of oxygen. Moreover, if the rate of corrosion of aluminum is indeed independent of electrode potential, as concluded, then the question of what is achieved by cathodic protection of aluminum must be raised. This question deserves further study, but one answer may be that cathodic protection influences the nature of the corrosion of aluminum without affecting the rate significantly. Cathodic protection may therefore prevent rapid pit initiation and propagation.

Figure 23 also illustrates that changes in the rates of the electrode processes accompany equilibration of the specimen with the solution. The fact that the rates of the cathodic and anodic processes are both lowered by continued exposure of the specimen to the solution suggests a common cause and may rule out concentration polarization. The limiting values of the cathodic and anodic current density can, therefore, be associated with the resistivity of the oxide film. The resistivity of the oxide film apparently increases with continued exposure of the specimen to the solution.

The hysteresis effects observed on repeated cathodic and anodic polarization can be rationalized in terms of the probable effects on the resistivity of the oxide film. The data in Figure 17

suggest that the film present on the aluminum after polarization has a greater resistivity than the initial film, if the circuit is opened between determinations. When the circuit is not opened between determinations, the film has a lower resistivity after polarization than the original film (Figure 18). The reduction in the rates evident in the anodic curves of Figures 19 and 20 can be similarly explained.

The rapid rise in current at -1.6 volts versus SCE in deaerated sodium chloride (-1.5 volts in the presence of oxygen) appears to be a characteristic feature of the polarization behavior of aluminum. Kunze states that the reaction shifts from the solution-metal oxide interface to the metal-metal oxide interface at that potential. In terms of the interpretation of the data presented here, however, a marked change in the resistivity of the film must take place at that potential, and it is suggested that the conduction through the oxide takes on an increasingly ionic character at potentials more active than -1.6 volts versus SCE, whereas conduction may be primarily electronic at higher potentials. The electrochemical behavior of aluminum at -1.6 volts versus SCE, therefore, has many features usually associated with a metal approaching the Flade potential, i.e., the potential which separates the passive from the active region of the anodic polarization curve (Point C in Figure 22).

The significance of the curves given in Figures 7 through 12 showing the variation of the corrosion potential with pH can now be explored. The above analysis of the polarization data at pH 4.0 has shown that the corrosion or mixed potential of aluminum

corresponds to the point of intersection of the self-polarization curves in the passive region. The corrosion potential at other values of the pH would be established in a similar way. Thus, to explain how the corrosion potential varies with pH, one would proceed to construct a series of corrosion diagrams similar to the one drawn in Figure 23 based on cathodic and anodic polarization data obtained over the entire pH range. A composite corrosion diagram could then be constructed which would not only give the corrosion potential - pH relationship, but would also provide estimates of the rate of corrosion as a function of pH in the given solution. The composite corrosion diagram envisaged would be the kinetic counterpart of the thermodynamic diagrams popularized by Pourbaix.

In the absence of the necessary data, the composite corrosion diagram given in Figure 24 has been constructed for freshly electropolished high-purity aluminum using an arbitrary procedure. The position of the curve at pH 0 was determined from hydrogen overvoltage data for aluminum in strongly acid solutions which indicate that the exchange current density is  $10^{-10}$  A/cm<sup>2</sup> and the slope of the current-voltage curve is -0.10.<sup>(2)</sup> The shape of the curve at pH 0 was drawn to conform to the shape of curve  $i_{c, 1}$  in Figure 23. The curve at pH 2.0 was placed halfway between the curves at pH 0 and pH 4.0. The remaining cathodic curves were then drawn parallel to the curves at pH 0, 2, and 4. The procedure is arbitrary, but it is not unreasonable to expect the hydrogen overvoltage to vary in some consistent fashion as drawn.

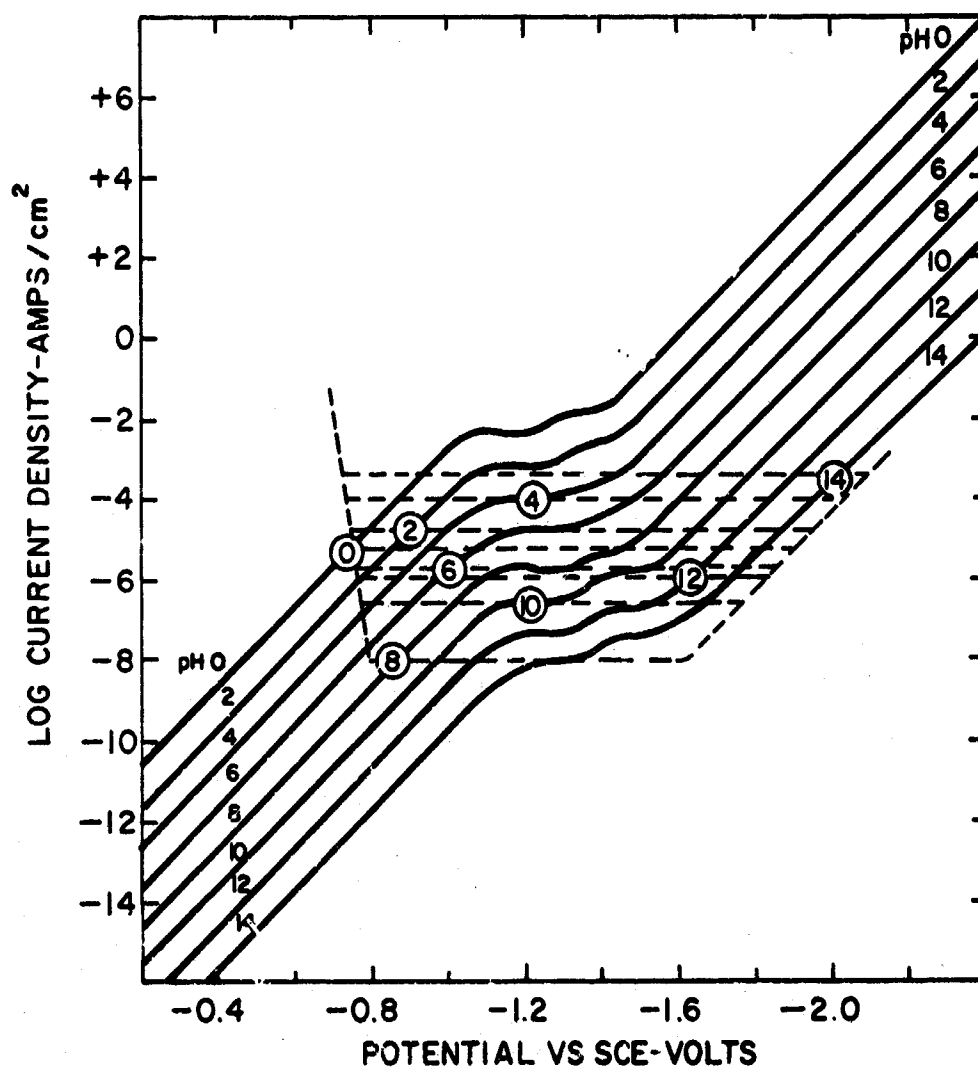


FIGURE 24 ESTIMATE OF THE CORROSION RATE - POTENTIAL - pH DIAGRAM OF ELECTROPOLISHED HIGH-PURITY ALUMINUM IN 0.5N SODIUM CHLORIDE

The anodic curves shown by the dotted lines in Figure 24 were estimated by marking the point on the appropriate cathodic curve of the experimentally determined corrosion potential at the corresponding pH. For example, the data in Figure 8 indicate that the corrosion potential of the high-purity aluminum in air-saturated 0.5N sodium chloride is -0.72 volt versus SCE at pH 0, and this point is indicated by the open circle on the cathodic curve marked pH 0 in Figure 24. The shape of the anodic curves is in accord with the conclusion that the rate of dissolution of aluminum is nearly independent of electrode potential over a broad range.

The corrosion potential - pH data are plotted in Figure 25. The solid line is a reasonable approximation of the data with the exception of some of the points obtained with etched specimens. The data can be approximated by three straight lines having slopes of -0.09, +0.10, and -0.18 in the low, intermediate and high range of pH. The slope of the corrosion potential - pH curve, -0.09 in the range pH 0 to 4, is approximately equal to the slope of the cathodic curves used to construct Figure 24. Thus, as Goudling and Downie have already found, the potential of pure aluminum varies with pH in the same manner as does the potential of a hydrogen electrode (in the pH range 0 to 3).<sup>(15)</sup> However, those authors report a slope of -0.059 which is higher than the value given above. From Figure 24, it is clear that slight changes in the rate of corrosion of aluminum will change the corrosion potential and the value of the slope. The value of the slope of the curve in Figure 25 in the

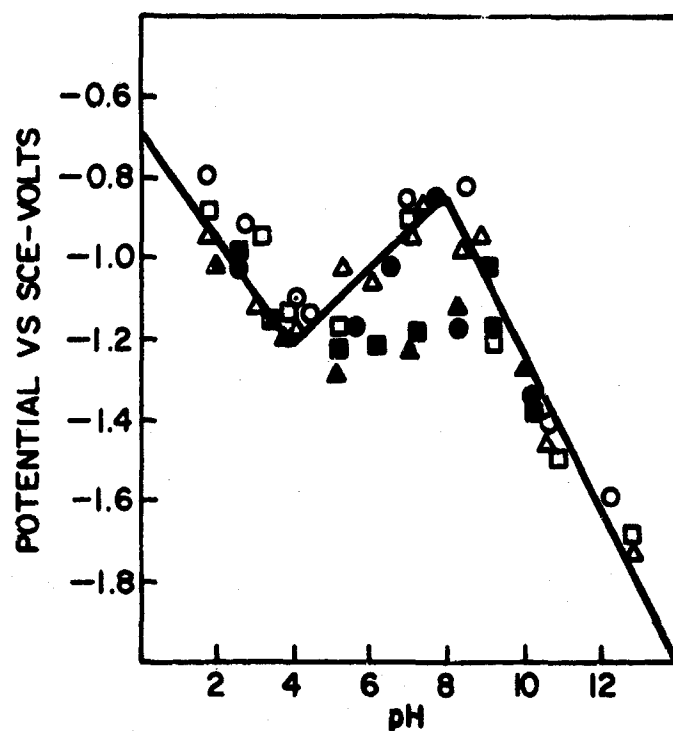


FIGURE 25 SUMMARY OF CORROSION POTENTIALS OF HIGH-PURITY ALUMINUM AS A FUNCTION OF pH: ELECTROPOLISHED SPECIMEN IN: □ 0.056N SODIUM SULFATE, △ 0.5N SODIUM CHLORIDE, ○ 0.056N SODIUM SULFATE AND 0.5N SODIUM CHLORIDE; ETCHED SPECIMENS IN: ■ 0.056N SODIUM SULFATE, ▲ 0.5N SODIUM CHLORIDE, AND ● 0.056N SODIUM SULFATE AND 0.5N SODIUM CHLORIDE

alkaline range is  $-0.18$  and appears to have little relation to the slope of the cathodic curves in Figure 24, but is in excellent agreement with the value of  $-0.1773$  predicted by Haynie and Ketcham.<sup>(11)</sup>

The variation of the rate of corrosion of aluminum with pH on the basis of the composite corrosion diagram (Figure 24) is given in Figure 26. The rate of corrosion increases in the pH range 0 to 4, decreases in the range 4 to 8, and increases in the range 8 to 14. The minimum at pH 8.0 may be the point at which the rate of formation of aluminum hydroxide on the electrode surface equals the rate of formation of the aluminate ion. The Pourbaix diagram for the aluminum-water reaction indicates these reactions are thermodynamically possible.<sup>(41)</sup> The formation and growth of aluminum hydroxide should act to reduce the rate of dissolution of aluminum, whereas aluminate ion formation should act to increase it. The rate of dissolution of aluminum should logically reach a minimum value at that pH where the rates of these two opposing reactions become equal.

The curve in Figure 26 is similar in shape to one determined by Vedder and Vermilyea by an entirely different experimental technique,<sup>(34)</sup> and this lends a measure of support to the interpretation of the electrochemical behavior of aluminum presented here.

The model for the dissolution of aluminum proposed by Vedder and Vermilyea places a great deal of emphasis on chemical factors, and they state that the rate of the corrosion reaction is controlled



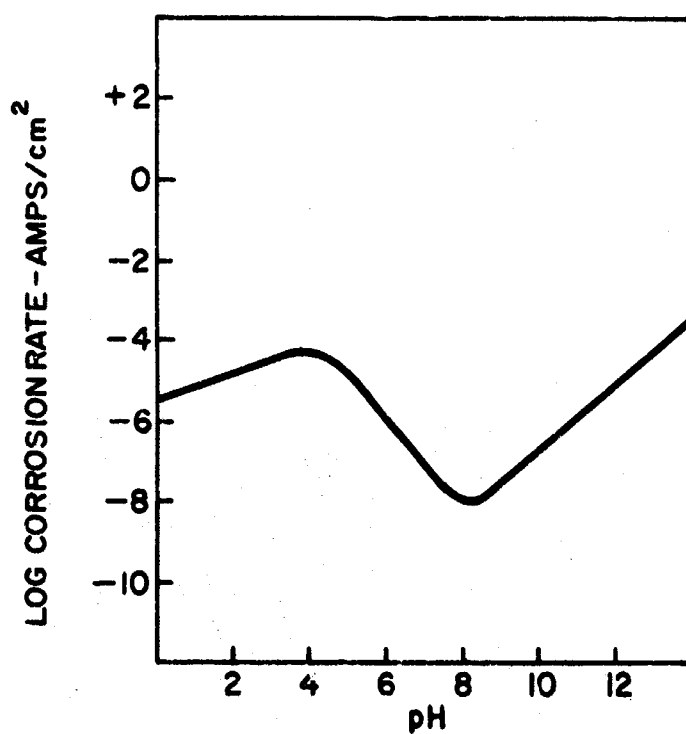


FIGURE 26 ESTIMATE OF THE INITIAL RATE OF DISSOLUTION OF HIGH-PURITY ALUMINUM AS A FUNCTION OF pH IN 0.5N SODIUM CHLORIDE

by the hydrolysis and dissolution of the barrier oxide film, and reprecipitation of aluminum hydroxide. However, the fundamental property affected by these chemical reactions appears to be the conductivity of the oxide, and conduction through the oxide may be the limiting factor. In fact, their suggestion that proton diffusion in the oxide may be an important factor is of interest. There should be an inverse relationship between the activity of aluminum interstitials and proton interstitials in the oxide. Assuming that the activity of the proton interstitials in the oxide is directly dependent on the activity of hydrogen ions in solution, one would expect the rate of corrosion of aluminum to increase with increasing pH as it does, except in the region where aluminum hydroxide precipitates. The role of proton diffusion in the corrosion of aluminum deserves further study.

#### Summary and Conclusions

The observations made during the controlled-potential weight-loss experiments strongly indicate that high-purity aluminum is an example of the stable passive state of metals. The implications of this have been examined. In the case of stable passive behavior, the experimentally determined anodic polarization curve should approach a limiting value indicative of the rate of corrosion of the metal. Extrapolating Tafel lines to the corrosion potential, the usual method of estimating the rate of corrosion of metals electrochemically, may give estimates of the rate of corrosion which are lower than the actual value for metals covered with oxide films.

The cathodic and anodic polarization data obtained in deaerated and air-saturated solutions of sodium chloride at pH 4.0 have been examined in terms of the above analysis. The limiting anodic current density value of the experimentally determined polarization curve has been used as the principal criterion of the rate of corrosion. Freshly electropolished high-purity aluminum initially displays a high rate of corrosion which decreases as the specimen is exposed to the solution. After periods greater than 24 hours, the rate of corrosion is of the order of  $10 \mu\text{A}/\text{cm}^2$ . The resistivity of the passive film increases with continued exposure of the specimen to the solution, and probable changes in the resistivity of the film have been used to explain the hysteresis effects observed on repeated polarization of the same specimen.

The self-polarization curves consistent with the experimental data at pH 4.0 have been constructed, and the curves clarify the process by which the mixed or corrosion potential is established on high-purity aluminum. The self-polarization curves for other values of pH have been estimated by a rather arbitrary procedure and used to construct a composite corrosion diagram which has been termed the kinetic analogue of the thermodynamic diagrams popularized by Pourbaix. The value of the composite diagram is that it gives both the corrosion potential and the corrosion rate as a function of pH. The composite corrosion diagram is consistent with the experimentally determined corrosion potential - pH relationships, and also provides estimates of the initial rate of corrosion of high-purity aluminum as a function of pH. The shape of the corrosion rate - pH curve

has been explained as the point at which the rate of formation of aluminum hydroxide on the electrode surface equals the rate of formation of the aluminate ion. Since these two reactions would have opposite effects on the corrosion reaction, a minimum should occur at that pH where the rates become equal. Although there is no question that chemical factors, such as the rate of dissolution of the barrier oxide film and the reprecipitation of aluminum hydroxide on the surface, are important in the dissolution of aluminum, the fundamental property affected by the chemical reactions appears to be the conductivity of the oxide. The effect of interstitial protons in the oxide has been briefly considered, and it has been suggested that the role of proton interstitials in the corrosion mechanism of aluminum be studied further.

Other conclusions are enumerated below:

1. The overvoltage for the reduction of oxygen on oxide-covered aluminum is high and, therefore, dissolved oxygen has a negligible effect on the rate of corrosion of high-purity aluminum. The predominant cathodic reaction occurring during the corrosion of aluminum is the reduction of hydrogen ions. Dissolved oxygen should have a greater effect on the rate of corrosion of alloys of aluminum than on high-purity aluminum.
2. The presence of dissolved oxygen increases the tendency for the high-purity aluminum to pit when cathodic potentials are applied, and it may be concluded that cathodic protection would be more

effective in the absence of oxygen. The cathodic protection of aluminum may help to control the nature of the attack on aluminum without significantly affecting the rate of dissolution.

3. The degree and extent of corrosion of high-purity aluminum varies with pH and is highly localized in character. Therefore, the average rate of corrosion as determined by electrochemical or other methods should be used with caution.
4. The electrochemical behavior of aluminum at -1.6 volts versus SCE has many features usually associated with a metal approaching its Flade potential, and it has been suggested that at potentials more active than -1.6 volts, conduction through the oxide takes on an increasingly ionic character, whereas at more noble values, conduction may be primarily electronic.

# BIBLIOGRAPHY

1. L. L. Shreir, "Principles of Corrosion and Oxidation." Chapter in Corrosion. Edited by L. L. Shreir. John Wiley and Sons, Inc., New York (1963).
2. H. H. Uhlig, Corrosion and Corrosion Control. John Wiley and Sons, Inc., New York (1965).
3. F. H. Haynie and W. K. Boyd, "Stress-Corrosion Cracking of Aluminum-Alloys," Defense Metals Information Center, DMIC Report No. 228, July 1, 1966.
4. G. A. DiBari, "Effect of Sulfur, Phosphorus, and Silicon on the Activity and Type of Corrosion of Nickel Anodes," Plating 53 (12), 1440 (1966).
5. David Gray and Allen Cahill, "Theoretical Analysis of Mixed Potentials," J. Electrochem. Soc. 116 (4), 443 (1969).
6. J. V. Petrocelli, V. Hospadaruk, and G. A. DiBari, "Electrochemistry of Copper, Nickel and Chromium in the Corrodokote and Cass Test Electrolytes," Plating 49 (1), 50 (1962).
7. G. A. DiBari and J. V. Petrocelli, "Effect of Composition and Structure on the Electrochemical Reactivity of Nickel," J. Electrochem. Soc. 112 (1), 99 (1965).
8. M. Stern, "Electrochemical Behavior of Iron in Oxygen-Free Acid Environments," J. Electrochem. Soc. 102, 609 (1955).
9. J. V. Petrocelli, "Electrochemistry of Dissolution Processes." Chapter in The Surface Chemistry of Metals and Semi-Conductors. Edited by H. C. Gatos. John Wiley and Sons, Inc. (1960).
10. J. Burke, The Kinetics of Phase Transformations in Metals. Pergamon Press, New York (1965).
11. F. H. Haynie and S. J. Ketcham, "Electrochemical Behavior of Aluminum Alloys Susceptible to Intergranular Corrosion. II. Electrode Kinetics of Oxide-Covered Aluminum," Corrosion 19 (12), 403t (1963).
12. F. N. Speller, Corrosion-Causes and Prevention. McGraw-Hill Book Company, Inc., New York (1951).
13. E. L. Koehler and S. Evans, "Pitting and Uniform Corrosion of Aluminum by pH 3.5 Citrate Buffer Solution," J. Electrochem. Soc. 111, (1), 17 (1964).

14. F. W. Fink, G. A. DiBari, F. H. Haynie, W. K. Boyd, and E. White, "Corrosion Control of Galvanically Incompatible Metals in Seawater," to be presented at the National Association of Corrosion Engineers Annual Conference, March 1971.
15. C. W. Goulding and T. C. Downie, "The Cathodic Polarization of Super-Purity Aluminum in Deaerated Acid Solutions and the Measurement of the Corrosion Rate," *Metallurgia* 68 (406), 93 (1963).
16. T. C. Downie and C. W. Goulding, "A Potentiostatic Examination of the Properties of Aluminum in Aqueous Solutions of Chlorides and Bromides," *Metallurgia* 73 (435), 45 (1966).
17. T. C. Downie and C. W. Goulding, "A Potentiostatic Examination of the Properties of Aluminum in Aqueous Solutions Containing Sulphate and Other Ions," *Metallurgia* 73 (436), 93 (1966).
18. J. W. Diggle, T. C. Downie, and C. W. Goulding, "Effect of Anodic Oxide Films on the Polarization of Aluminum," *Corrosion Science* 8, 907 (1968).
19. D. A. Jones, "Anodic Polarization of Anodized Aluminum," *Corrosion* 25 (4), 187 (1969).
20. J. V. Petrocelli, "The Electrochemical Behavior of Aluminum I. In Solutions of Cerium Sulfate in Sulfuric Acid," *J. Electrochem. Soc.*, 97 (1), 10 (1950).
21. J. V. Petrocelli, "The Electrochemical Behavior of Aluminum II. In Solutions of Iron Sulfate," *J. Electrochem. Soc.*, 98 (5), 183 (1951).
22. J. V. Petrocelli, "The Electrochemical Behavior of Aluminum," *J. Electrochem. Soc.*, 99 (12), 513 (1952).
23. J. Kunze, "Untersuchungen Zur Elektrochemischen Polarisierung Von Aluminum in Gepufferter Natriumchloridlosung," *Corrosion Science* 7, 273 (1967).
24. J. C. Bailey and F. C. Porter, "Aluminum and Aluminum Alloys." Chapter in *Corrosion*, Volume 1. Edited by L. L. Shreir. John Wiley and Sons, Inc., New York (1963).
25. W. Beck, F. G. Keihn, and R. G. Gold, "Corrosion of Aluminum in Potassium Chloride Solutions. I. Effects of Concentrations of KCl and Dissolved Oxygen," *J. Electrochem. Soc.*, 101 (8), 393 (1954).
26. W. H. Ailor, Jr., "Evaluation of Aluminum After One-Year Deep Sea Exposure," *J. of Hydronautics* 2 (1), 26 (1968).

27. F. M. Reinhart, "Corrosion of Materials in Surface Sea Water After 6 Months of Exposure," Technical Note N-1023, Naval Civil Engineering Laboratory, Port Hueneme, California, (March 1969).
28. E. T. Wanderer and M. W. Wei, "Applicability of Aluminum for Desalination Plants," *Metals Engineering Quarterly*, 7 (3), 30 (1967).
29. V. H. Troutner, "Observations on the Mechanism and Kinetics of Aqueous Aluminum Corrosion, Part 1, Role of the Corrosion Product Film in the Uniform Aqueous Corrosion of Aluminum," *Corrosion*, 15 (1), 9t (1959).
30. M. S. Hunter and P. Fowle, "Natural and Thermally Formed Oxide Films on Aluminum," *J. Electrochem. Soc.*, 103 (9), 482 (1956).
31. M. J. Dignam, "Oxide Films on Aluminum. I. Ionic Conduction and Structure," *J. Electrochem. Soc.*, 109 (3), 184 (1962). "II. Kinetics of Formation in Oxygen," *J. Electrochem. Soc.*, 109 (3), 192 (1962).
32. R. L. Dillon, "Observations on the Mechanisms and Kinetics of Aqueous Aluminum Corrosion, Part 2. Kinetics of Aqueous Aluminum Corrosion," *Corrosion* 15 (1), 13t (1959).
33. M. A. Heine and M. J. Pryor, "The Distribution of A-C Resistance in Oxide Films on Aluminum," *J. Electrochem. Soc.*, 110 (12), 1205 (1963).
34. W. Vedder and D. A. Vermilyea, "Aluminum Water Reactor," *Trans. Faraday Soc.*, 65, 561 (1969).
35. D. A. Vermilyea, "The Dissolution of MgO and Mg(OH)<sub>2</sub> in Aqueous Solutions," *J. Electrochem. Soc.*, 116 (9), 1179 (1969).
36. R. K. Hart, "The Oxidation of Aluminum in Dry and Humid Oxygen Atmospheres," *Proc. Roy. Soc., (A)* 236, 68 (1956).
37. C. G. Dunn and L. A. Harris, "Auger Electron Analysis of Electropolished High-Purity Aluminum," *J. Electrochem. Soc.*, 117 (1), 81 (1970).
38. R. B. Mears, "Aluminum and Aluminum Alloys," Chapter in Corrosion Handbook. Edited by H. H. Uhlig. John Wiley and Sons, Inc., New York (1948).
39. J. M. Bryan, "Aluminum and Aluminum Alloys in the Food Industry," pp. 43, 55, His Majesty's Stationary Office, London (1948).



40. R. L. Davies, Iron Street Institute Spec. Rep. 45, 131 (1952).
41. E. Deltombe and H. Pourbaix, "The Electrochemical Behavior of Aluminum," Corrosion 14 (11), 496t (1958).


## VITA

George A. DiBari was born in Brooklyn, New York, on February 8, 1934. Upon graduation from Fort Hamilton High School in June, 1951, he attended Brooklyn College, receiving his Bachelor of Science degree in Chemistry in June, 1955.

He has worked as a chemist for the Curtiss Wright Corporation, Wright Aeronautical Division, Woodridge, New Jersey and as a research chemist for the International Nickel Company, Inc., Paul D. Mercia Research Laboratory, Sterling Forest, Suffern, New York. He received his Master of Science degree in Chemistry from the Polytechnic Institute of Brooklyn in June, 1963.

He joined the staff of The Pennsylvania State University, Ordnance Research Laboratory, as a research assistant in January, 1967, and has been concerned with development and research activities dealing with the corrosion protection of naval ordnance.

The author is a member of the Electrochemical Society, the American Electroplaters' Society, and the National Association of Corrosion Engineers. He received his undergraduate degree cum laude, and is a member of the Phi Kappa Phi Honor Society.

DOCUMENT CONTROL DATA - R & D		
(Security classification of title, abstract and indexing annotation when overall report is classified)		
1. ORIGINATING ACTIVITY (Corporate author)		2a. REPORT SECURITY CLASSIFICATION
Ordnance Research Laboratory University Park, Pennsylvania		Unclassified
3. REPORT TITLE		2b. GROUP
The Electrochemical and Corrosion Behavior of Aluminum		
4. DESCRIPTIVE NOTES (Type of report and inclusive dates)		
Ph.D. Thesis      December, 1970		
5. AUTHOR(S) (First name, middle initial, last name)		
George A. Di Bari		
6. REPORT DATE	7a. TOTAL NO. OF PAGES	7b. NO. OF REFS
June 18, 1970	82 pages and figures	41
8a. CONTRACT OR GRANT NO.	9a. ORIGINATOR'S REPORT NUMBER(S)	
N00017-70-C-1407	TM 703-02	
b. PROJECT NO.	9b. OTHER REPORT NO(S) (Any other numbers that may be assigned this report)	
c.		
d.		
10. DISTRIBUTION STATEMENT		
Distribution of this document is unlimited.		
11. SUPPLEMENTARY NOTES		12. SPONSORING MILITARY ACTIVITY
None		Naval Ordnance Systems Command Department of the Navy
13. ABSTRACT		
<p>    The electrochemical behavior of high-purity aluminum has been studied to clarify the corrosion behavior of the metal when exposed to oxygen-free and oxygen-saturated saline solutions of varying pH. The mixed or corrosion potential, <math>E_M</math>, of the electropolished high-purity aluminum decreases as the pH is increased except in the intermediate pH range (4 to 8) where <math>E_M</math> increases. A local maximum in the corrosion potential curve as a function of pH is thus observed. Potentiostatic polarization data obtained at pH 4.0 suggest that the rate of dissolution of high-purity aluminum is nearly independent of electrode potential over a fairly wide range, relatively insensitive to the presence of dissolved oxygen in the electrolyte, and highly sensitive to changes in pH. Dissolved oxygen influences the type of corrosion when cathodic potentials are applied. Based on the potentiostatic data, a corrosion diagram believed to be valid for sodium chloride solutions from pH 0 to pH 14 has been constructed. The corrosion diagram is consistent with the observed relation between <math>E_M</math> and pH, and also yields estimates of the rate of dissolution of aluminum as a function of pH. The results appear to be consistent with the Pourbaix Diagram for the aluminum-water reaction and with the dissolution-precipitation mechanism for the dissolution of aluminum recently proposed by Vedder and Vermilyea. </p>		

14.	KEY WORDS	LINK A		LINK B		LINK C	
		ROLE	WT	ROLE	WT	ROLE	WT
	Electrochemistry	8					
	Corrosion	8					
	Aluminum	8					
	pH Effects	8					
	Salinity	8					